be delivered only after a delay of several years, if at all. This is unfair to the authors who deliver their articles promptly, only to see them appear years later when they have become dated, as the relevant volumes finally acquire their full complement of articles, or after the editors have despaired of achieving this full complement.

In order to overcome these problems, I recommended to the publishers the establishment of this new journal, FUNDAMENTALS OF COSMIC PHYSICS. This is to be a journal that aims at publishing handbook-type articles. Hence the authors will not be penalized by unduly long delays. It is true that the articles will not come to the reader neatly packaged into units dealing with related topics, as in a true handbook series. However, related articles can be collected and reprinted in hard covers, and the occasional very lengthy article can appear as a separate monograph. In this way the journal format possesses considerable flexibility.

The principal way in which a handbook article should differ from a review article is in its degree of internal completeness. A review article indicates the current status of research in a field and serves as a guide to the literature. A handbook article should contain derivations of important results and its coverage of the field should be sufficiently complete so that only professional workers in that field would ordinarily have to go beyond the article to the original literature. The handbook article should be readily understandable by graduate students. These goals of the handbook article are more difficult to achieve than those of the review article, and authors will have a variable success in meeting them. However, the extra effort involved should result in articles which have an enduring impact on the consolidation of knowledge in cosmic physics.

The term 'cosmic physics' includes general relativity and gravitation, astronomy and astrophysics, space and planetary physics, and geophysics. A board of associate editors has been established with a distribution among these fields; the associate editors suggest topics for articles and possible authors. Those who may be interested in contributing articles should first contact the editor, in order that it may be determined whether the suggested article will fit into the framework of the other articles which have been solicited. The membership of the board of associate editors will be rotated from time to time.

Publication of this journal will be irregular, in response to the flow of manuscripts.

A.G.W. CAMERON

Fundamentals of Cosmic Physics; 1973, Vol.1, pp.1–70

Printed in Great Britain

The Evolution of Protostars — Theory

R. B. LARSON
Yale University Observatory, New Haven, Connecticut 06520, U.S.A.

1 INTRODUCTION: THE PROBLEM OF STAR FORMATION

Modern ideas on star formation date back to Newton (1692), who first suggested that stars might form through gravitational condensation of diffuse matter in space. Since Newton's time this general idea has become widely accepted as basically correct; nevertheless, the problem of just how star formation occurs has remained a matter for speculation and even controversy. In recent years, substantial new developments in both theory and observation have begun to throw new light on various aspects of the star formation process and to provide strong confirmation that stars are presently forming by gravitational collapse processes in dense interstellar clouds. While our understanding of star formation is still far from complete, some of the principal features of the collapse process can now be outlined with reasonable confidence, and various stages of the collapse appear to be identifiable with certain types of observed objects, such as some dark globules, some infrared objects, and the T Tauri stars.

The earliest stages of the star formation process, including the formation of interstellar clouds which are massive and dense enough to be gravitationally bound, are at present somewhat less certain; both thermal and magnetic instabilities have been suggested as playing a role in causing the interstellar medium to condense into clouds. The fact that star formation is concentrated in spiral arms indicates that some large scale dynamical phenomenon such as a galactic shock or compression wave must also play a role. In any case, it is clear from observations that there exist dark clouds and globules in which the density is sufficiently high that self gravitation is important and collapse into stars seems likely to occur. In this article we shall take as our starting point, and we shall be concerned only with those stages of the star formation process following the appearance of a gravitationally bound cloud or 'protostar'. For a more general review of the various problems associated

with star formation and of the relevant properties of the interstellar medium the reader is referred to the comprehensive discussions by Spitzer (1968, a, b) and to the shorter review articles by Field (1970) and Penston (1971). For a more skeptical point of view on theories of star formation, the reader may consult the review article by McNally (1971).

We shall be concerned in this article with the evolution of a protostar, which we define as a cloud or aggregate of interstellar material which is gravitationally bound and is collapsing or about to collapse into a star. This presupposes, of course, that a protostar is a well defined object and is distinct from its surroundings. In reality a protostar may not have any well defined boundary but may merge continuously with its surroundings; furthermore, it may not even have a well defined mass, since it may exchange material with its surroundings. Thus the concept of a 'protostar' as defined above is clearly an idealization, and theoretical models which treat protostars as isolated objects are likewise idealized. Nevertheless, such approximations are at present necessary to make the theory tractable, and they do not necessarily invalidate the results, provided that the limitations are kept in mind.

The present article will not treat the purely hydrostatic phases of pre-main sequence evolution, a subject which has already been extensively discussed elsewhere; for a recent comprehensive review, the reader is referred to the article by Bodenheimer (1972).

2 THE JEANS CRITERION AND THE INITIAL STATE OF A PROTOSTAR

If a dense cloud or condensation of interstellar matter is to collapse gravitationally into a star or group of stars, its self gravitation must be strong enough to overcome the forces tending to disperse the cloud and prevent collapse. The forces tending to support or disperse the cloud will in general include (1) the thermal gas pressure, (2) magnetic pressure, (3) centrifugal force if the cloud is rotating, and (4) the effects of internal turbulent motions. It is generally argued that internal turbulent motions will probably not be very important, since their importance will exceed that of thermal pressure only if the turbulence is supersonic, and supersonic turbulence is expected to decay in a time shorter than the free fall time of the cloud. This argument neglects the fact that the turbulent motions will tend to be amplified by the collapse process itself, and therefore it is not clear that turbulent motions can be completely dismissed as unimportant for the collapse. However, as far as the initial conditions are concerned, any turbulent motions may be considered as simply adding an extra contribution to the thermal pressure. We shall discuss first the role of the thermal or turbulent pressure in determining the initial conditions for a collapsing

protostar, leaving to later sections a consideration of the effects of rotation and magnetic fields.

The conditions under which self gravitation will dominate over pressure forces and cause collapse to occur are determined by the Jeans criterion, which can be derived and stated in a number of ways (Spitzer 1968a). In essence, the Jeans criterion simply states that in order for collapse to occur, the gravitational potential energy of a cloud must be comparable to or greater than the kinetic energy of thermal or turbulent motions within the cloud. (A very similar result is obtained from the virial theorem, which states that in order for an *isolated* configuration to collapse, its gravitational potential energy must exceed twice its kinetic energy.) For a cloud of mass M, radius R, and temperature T, the gravitational potential energy per unit mass is approximately $(3/5)GM/R$, whereas the thermal kinetic energy per unit mass is $(3/2)\mathcal{R}T$ where $\mathcal{R} = k/\mu H$ is the gas constant for the cloud material (here μ is the mean molecular weight, and H is the mass of the hydrogen atom). Thus in order for collapse to occur we must have

$$\frac{GM}{R} \gtrsim \frac{5}{2}\mathcal{R}T \,. \tag{1}$$

If, for example, we consider a cloud of given mass and temperature, the Jeans criterion states that it can collapse gravitationally if its radius is equal to or less than a critical value of approximately $(2/5)GM/\mathcal{R}T$. For a more precise derivation of the numerical constant in the Jeans criterion one can, for example, assume that the cloud begins as an equilibrium isothermal sphere and is slowly compressed to the point where stable equilibrium is no longer possible; this yields a critical radius of

$$R_c = 0.41\,\frac{GM}{\mathcal{R}T} \tag{2}$$

(Spitzer 1968a). Another approach, which may be more realistic, is to suppose that the cloud is never in equilibrium but collapses isothermally from an initial configuration of uniform density; if, for example, the outer boundary of the collapsing cloud is held fixed (see Section 4), one then finds from trial collapse calculations that collapse to a star can occur only if the radius is less than a maximum value

$$R_m = 0.46\,\frac{GM}{\mathcal{R}T} \tag{3}$$

(Larson 1969a).

The Jeans criterion can also be written to give the minimum mass M_J which a cloud of given density and temperature must have in order to collapse gravitationally; for example, the minimum unstable mass M_J implied by Eq. (2) is

$$M_J = 1.86\,\rho^{-1/2}\,(\mathcal{R}T/G)^{3/2} \qquad (4)$$

It has long been realized that for typical interstellar clouds the minimum unstable mass predicted by the Jeans criterion is of the order of $10^3\ M_\odot$ or more, which means that stars in the normal mass range cannot form directly by gravitational collapse in typical interstellar clouds. If stars of normal mass are to form, densities several orders of magnitude higher than those normally encountered in the interstellar medium are required. Even under the conditions of strong compression proposed for galactic density wave shocks, the minimum cloud mass for which gravitational collapse can occur is $\sim 120\ M_\odot$ (Shu *et al.* 1972). It is therefore generally believed that star formation begins with a cloud of relatively large mass ($\approx 10^3\ M_\odot$) which collapses gravitationally and fragments into smaller masses as its density rises and the Jeans mass M_J decreases. By 'fragmentation' we refer here to the development within the cloud of subcondensations which are gravitationally bound and which begin to collapse on themselves. Several stages of fragmentation may occur, leading eventually to the formation of protostars of one solar mass.

At each stage of the fragmentation process the size of the condensations which form is governed or at least limited by the Jeans criterion, which gives the minimum mass that a subcondensation of given density and temperature must have if it is to collapse. While the Jeans criterion says nothing about the *maximum* mass that a subcondensation can have, numerical collapse calculations such as those to be described below suggest that a condensation much larger than the Jeans mass is not likely to collapse very far without fragmenting into smaller condensations. The reason for this is that the free fall time varies as $\rho^{-1/2}$, so that denser regions always collapse fastest and any small density fluctuations are rapidly amplified, provided that their masses exceed the Jeans mass. Thus if a cloud whose mass is much larger than the Jeans mass contains any small density variations, these will soon develop into subcondensations with masses closer to the Jeans mass. Therefore we expect that protostars formed by such a fragmentation process should have sizes and masses which are roughly consistent with the Jeans criterion, at least in order of magnitude.

Evidence for the type of fragmentation process sketched above is provided by observations of a number of dark clouds showing internal structure, such as the Southern Coalsack and the dark cloud near ρ Ophiuchi (Bok *et al.* 1971); these are dense, massive clouds with masses of the order of $10^3\ M_\odot$ which are probably gravitationally bound and beginning to collapse and

fragment into stars. Some smaller and more filamentary dark clouds, which are also probably gravitationally bound, are observed in the Taurus region. In all of these cases the dark clouds have a conspicuously clumpy internal structure, just as would be expected if they are undergoing gravitational collapse and fragmentation. In many cases the subcondensations or globule-like structures seen in these clouds have properties which, within the uncertainties, appear to be consistent with the Jeans criterion and to resemble closely the initial conditions assumed for the protostar models to be described below. The properties of some of the more isolated dark globules, which also resemble the theoretical protostar models in many cases, have been described by Bok *et al.* (1971).

The above discussion has assumed that protostars form by purely gravitational collapse and fragmentation processes, starting with a cloud of sufficiently large mass. However, it is also possible that under some circumstances protostars can form as a result of thermal instabilities in a medium which is cooling from high temperatures (Hunter 1969, Stein *et al.* 1972). In fact, Stein *et al.* (1972) propose that protostars with masses as small as one solar mass or less can form directly out of the interstellar medium without the need for any fragmentation process, and they suggest that this may explain some of the Bok globules. While the initial conditions for such protostars are rather different from those derived from the Jeans criterion, the early stages of evolution exhibit some strong qualitative similarities in the two cases (Stein *et al.* 1972). Thus, while we shall continue to discuss the evolution of protostars on the assumption that they are formed by gravitational collapse and fragmentation processes, some of the basic qualitative results may remain valid even for the case of protostars which are formed by thermal instabilities.

3 THE TEMPERATURE OF THE PROTOSTELLAR MATERIAL

As may be seen from Eq. (4), the temperature of the protostellar material plays an important role in determining the initial conditions for collapsing protostars. The temperature of the protostellar material can be estimated by considering the balance between the various heating and cooling processes thought to be important, as is customarily done in calculating the temperature of interstellar matter. In the case of protostars, the relevant densities are so high ($\gtrsim 10^{-20}$ to 10^{-18} g cm^{-3}) that the protostar is opaque to visual and ultraviolet radiation, and the important heating and cooling processes are different from those usually considered for the interstellar medium. A detailed treatment of the heating and cooling rates would be quite complicated, particularly in the transition region between optically

thin and optically thick conditions; however, since the temperature is not very sensitive to the details, a simplified approximate treatment will suffice to determine the temperature with reasonable accuracy. We shall consider the effects of heating by cosmic rays and by gravitational compression, and cooling by C II, O I, and dust grains; while many other processes operate, these appear to be the dominant processes under protostellar conditions. More elaborate treatments of the heating and cooling processes in protostars, based on slightly different assumptions than those used here, have been given by Nishida (1968) and by Hattori *et al.* (1969), but the results are not greatly different from those obtained here.

It has been suggested that low energy cosmic rays may be the most important source of heating in the interstellar medium, and a cosmic ray heating rate of 2.5×10^{-3} erg g^{-1} s^{-1} has been adopted by Goldsmith *et al.* (1969). In a dense protostellar cloud these low energy cosmic rays are subject to significant absorption, the opacity being approximately 300 cm^{2}g^{-1} (Spitzer and Scott 1969), about the same as the opacity to visual radiation. For simplicity we shall assume that cosmic rays and visual radiation are both attenuated by the same factor $e^{-\tau}$ where τ is the optical depth at the center of the cloud. The cosmic ray heating rate is then

$$\Gamma_{CR} = 2.5 \times 10^{-3}\, e^{-\tau} \text{ erg g}^{-1} \text{ s}^{-1} . \tag{5}$$

When τ becomes much larger than unity, cosmic ray heating becomes unimportant, as does heating by ultraviolet radiation. The most important heating mechanism in a collapsing cloud then becomes compressional heating. For a cloud or fluid element which is collapsing at the free fall rate the compressional heating rate is $P\,dV/dt = (24\pi G\rho)^{1/2}\, \mathcal{R}T$ erg g^{-1} s^{-1} ($V = 1/\rho$). Since the numerical collapse calculations show that finite pressure gradients cause the collapse to be somewhat retarded from a free fall, we shall assume that heating occurs at half the free fall rate; then, adopting $\mathcal{R} = 3.36 \times 10^7$ erg g^{-1} °K^{-1}, as is appropriate for a composition of mostly H_2 (Gaustad 1963), we have for the compressional heating rate

$$\Gamma_f = 3.8 \times 10^4\, \rho^{1/2}\, T \text{ erg g}^{-1} \text{ s}^{-1} . \tag{6}$$

In typical interstellar clouds, cooling is thought to occur mainly through collisional excitation of C II ions by H atoms, followed by the emission of infrared photons. In an opaque cloud, the cooling rate due to this process is reduced because the ultraviolet radiation that produces the C II ions is absorbed. Assuming that only $\frac{1}{10}$ of the carbon in the interstellar medium is available in gaseous form and that the C II abundance is further reduced by a factor $e^{-\tau}$ in an opaque cloud, the C II cooling rate is

$$\Lambda_{CII} = 9.0 \times 10^{19}\, e^{-\tau}\, \rho\, e^{-92/T} \text{ erg g}^{-1} \text{ s}^{-1} \tag{7}$$

(Goldsmith *et al.* 1969). A second collisional excitation process which may contribute to the cooling of dense clouds involves excitation of O I atoms by H atoms; the cooling rate for this process is

$$\Lambda_{OI} = 2.5 \times 10^{20}\, \rho\, T^{0.33}\, e^{-228/T} \text{ erg g}^{-1} \text{ s}^{-1} \tag{8}$$

(Goldsmith *et al.* 1969).

In very dense, opaque, cold clouds, both of the above cooling processes become ineffective and cooling is produced mainly by inelastic collisions between gas molecules and dust grains, followed by the emission of infrared radiation from the grains. Assuming that the hydrogen in very dense clouds is all in molecular form (Hollenbach *et al.* 1971) and that each gram of material contains 2×10^{11} dust grains of radius 2×10^{-5} cm (Gaustad 1963), the rate of transfer of energy from the gas to the dust grains is given by

$$\Lambda_g = 1.1 \times 10^{14}\, \rho\, T^{1/2}\, (T - T_g) \text{ erg g}^{-1} \text{ s}^{-1} \tag{9}$$

where T is the gas temperature and T_g the grain temperature. It has been assumed in deriving this relation that the colliding gas molecules leave the grains with a kinetic energy corresponding to the grain temperature. The grain temperature is determined by the balance between heating at the above rate and cooling by the thermal emission of far infrared radiation which escapes freely from the cloud. The emission rate per gram of material is given by

$$j = 2.3 \times 10^{-4}\, \kappa_P T_g^4 \text{ erg g}^{-1} \text{ s}^{-1} \tag{10}$$

where $\kappa_P(T_g)$ is the Planck mean opacity produced by dust grains. In the relevant temperature range, the Planck mean opacity has been estimated to be about $3 \times 10^{-5}\, T_g^3$ cm^2 g^{-1} (Hayashi and Nakano 1965); although this value is quite uncertain, the error is not very important, owing to the strong dependence of j on T_g.

The temperatures of both the gas and the dust can now be estimated by equating the heating and cooling rates for the gas and the dust:

$$\Gamma_{CR} + \Gamma_f = \Lambda_{CII} + \Lambda_{OI} + \Lambda_g \tag{11}$$

$$\Lambda_g = j . \tag{12}$$

Some temperatures calculated from these equations are listed in Table I for clouds of two masses, $1\, M_\odot$ and $10^3\, M_\odot$. The optical depths τ appearing in Eqs (5) and (7) have been calculated on the assumptions that the cloud has

uniform density (which is no longer true after gravitational collapse has started) and that the opacity to both cosmic rays and ultraviolet radiation is the same as the visual opacity, taken to be 250 $cm^2\ g^{-1}$. At the lowest densities, i.e. below about 3×10^{-20} g cm^{-3} for a $1\ M_\odot$ cloud and 3×10^{-21} g cm^{-3} for a $10^3\ M_\odot$ cloud, cosmic ray heating and C II cooling are the dominant processes. Since the rates for both processes depend in the same way on the optical depth τ , the temperature is almost independent of the size or optical depth of the cloud. The temperature at these low densities is, however, sensitive to the assumed abundances of the principal coolants C II and O I; for example, if all of the carbon is in gaseous form instead of only 10% as we have assumed, the temperatures at the lowest density listed would be reduced to about 20°K.

TABLE I

Equilibrium temperatures in dense clouds

	$M = M_\odot$		$M = 10^3\ M_\odot$	
log ρ (g cm^{-3})	τ	T(°K)	τ	T(°K)
− 22	4.2(−2)	50.6	4.2(−1)	48.1
− 21	2.0(−1)	25.4	2.0(+0)	24.6
− 20	9.1(−1)	15.6	9.1(+0)	16.3
− 19	4.2(+0)	8 4	4.2(+1)	6 6
− 18	2.0(+1)	5.1	2.0(+2)	5.1
− 17	9.1(+1)	5.4	9.1(+2)	5.4
− 16	4.2(+2)	6.3	4.2(+3)	6.3
− 15	2.0(+3)	7.5	2.0(+4)	7.5
− 14	9.1(+3)	9.1	9.1(+4)	9.1
− 13	4.2(+4)	11.0	4.2(+5)	11.0
− 12	2.0(+5)	13.3	2.0(+6)	13.3

At densities higher than about 3×10^{-20} g cm^{-3} , cosmic ray heating and C II cooling both become unimportant and the dominant processes become compressional heating and grain cooling. At densities above 10^{-19} g cm^{-3} the gas temperature becomes closely coupled to that of the dust grains. Since the infrared emissivity of the dust varies approximately as T_g^7 , the dust temperature depends only weakly on the density and the compressional heating rate, and is not very sensitive to the amount or the composition of the dust. Consequently a dense collapsing protostellar cloud should have a fairly well determined temperature of the order of 10°K, as given by Table I. From Table I we see that the temperature remains between about 5 and 11°K over the entire density range from the density at which a protostar becomes gravitationally bound and starts to collapse on itself ($\sim 10^{-19}$ g cm^{-3} for a protostar of one solar mass) to the density at which the central part of the

protostar becomes opaque to the infrared radiation from the dust grains ($\sim 10^{-13}$ g cm^{-3}). Thus it should be a fairly realistic approximation to assume, as has often been done, that the early stages of the collapse of a protostar are isothermal; the average temperature suggested by Table I is then about 8°K. The approximately isothermal nature of the collapse is verified by the detailed hydrodynamical calculations of Hunter (1969), Penston (1969 b), and Disney *et al.* (1969), in which the heating and cooling processes are explicitly included, although these authors all employed somewhat different treatments of these processes.

Temperatures closely comparable with the predicted temperatures are observed in many of the dense dark clouds in which star formation is believed to occur (Heiles 1971). The densities in these clouds are of the order 10^{-20} g cm^{-3} or higher, and the temperatures inferred from radio observations range from about 5°K to 20°K, a typical value being about 10°K. The good agreement between predicted and observed temperatures strengthens the conclusion that during its early development a protostar of one solar mass is approximately isothermal with a temperature of the order of 10°K. (Note, however, that because of the lower densities implied by the Jeans criterion for the more massive protostars, somewhat higher initial temperatures may be more appropriate for massive protostars; see the following section.)

4 INITIAL AND BOUNDARY CONDITIONS FOR A COLLAPSING PROTOSTAR

In order to compute the collapse of a protostar, it is necessary to specify not only the initial temperature but also the initial density and velocity at each point in the cloud. If the temperature is assumed known, the Jeans criterion gives the minimum density or equivalently the maximum radius which a cloud of given mass must have if it is to collapse gravitationally. It is difficult to give a more detailed specification of the initial conditions, however, since this depends on the poorly understood previous history of the material which makes a protostar, and also on the exact time chosen as the initial instant for the collapse, which is somewhat arbitrary. Because of the uncertainty in the initial conditions, a variety of different assumptions have been experimented with by workers in the field (see, for example, Penston 1966, Bodenheimer and Sweigart 1968, Larson 1969a).

With regard to the initial density distribution, one assumption which has been tried is that the initial state is close to a hydrostatic equilibrium configuration, either isothermal or polytropic. This presupposes that the conditions preceding the collapse of a protostar are sufficiently quiescent to allow approximate hydrostatic equilibrium to be established; however, it is not clear whether this situation will ever be closely approached inside a collapsing

and fragmenting interstellar cloud. At the opposite extreme, it has been assumed that no approach to hydrostatic equilibrium is ever achieved during the fragmentation process and that a protostar begins its collapse from a state of uniform density with no central concentration. Fortunately, the results of the collapse calculations show that the collapse always proceeds in much the same way regardless of the exact choice of initial density distribution. Thus, for example, even if the density of the protostar is initially uniform, the density distribution soon develops a centrally condensed structure which is almost indistinguishable from that found during the collapse of a cloud which was centrally condensed to begin with. Since the exact choice of initial density distribution is not very important for the collapse, most of the calculations to be described in this article have adopted the simplest possible assumption, i.e. an initially uniform density distribution.

The initial velocity distribution is also difficult to specify in any detail without a better understanding of how protostars are formed. Most calculations have assumed that a protostar begins its collapse from a state of rest, but calculations have also been made with the assumption that a protostar is initially expanding or contracting at approximately the free fall rate. As with the initial density distribution, the assumed initial velocity distribution does not make a great deal of difference to the behaviour of a collapsing cloud; once the collapse gets well under way the details of the initial conditions are largely forgotten and the interior part of the cloud collapses in much the same way, regardless of the assumed initial velocity distribution. (This conclusion requires modification if the cloud is rotating, rather than merely expanding or contracting; see Section 7.)

In addition to the initial conditions, it is also necessary to specify the boundary condition for a collapsing protostar. The boundary condition is even more difficult to specify than the initial conditions, since it depends on the properties of the surrounding medium and on the interactions between a protostar and its surroundings. Indeed, it is not even clear that one can unambiguously define a 'boundary' for a protostar, since the protostar may merge continuously with its surroundings, and it may not be clear initially how much of the material will collapse into a star. Nevertheless, for computational purposes it is necessary to choose a boundary and to specify either the velocity with which it moves or the pressure exerted on it by the surrounding material. One possibility that has been considered is that the surrounding medium continues to exert a constant pressure on the boundary of the protostar; in this case the boundary contracts with time, although not as rapidly as the interior of the cloud which still becomes strongly centrally condensed. At the other extreme, one can assume that the protostar is surrounded by a vacuum and that there is zero pressure on its boundary; in this case the boundary expands while the inner part of the cloud contracts. A third possibility, representing a compromise between these extreme cases, is that

the boundary pressure remains just sufficient to prevent the boundary from expanding but not sufficient to make it contract, so that the boundary remains stationary. As was the case with the initial conditions, it is found that once the collapse gets well under way the interior part of the cloud collapses in much the same way in all cases, regardless of the exact choice of boundary condition. Because of this, most of the collapse calculations to be described have adopted the simplest assumption, i.e. that the boundary remains stationary; this corresponds to allotting a fixed volume to each collapsing protostar in a forming protocluster.

While the principal qualitative features of the collapse are very similar in all cases, there are, of course, quantitative differences in the time scales and other results obtained with different initial and boundary conditions. These differences can cause a significant uncertainty or scatter in the properties of protostars and newly formed stars; see Section 16.

For the case of an initially uniform spherical cloud which collapses isothermally within a fixed boundary, the Jeans criterion is given by Eq. (3). For numerical reasons, in order to avoid having the collapse stopped and reversed by small numerical errors, the collapse calculations of Larson (1969a, 1972b) have instead used Eq. (2) which gives a slightly smaller radius and higher density than Eq. (3). For a protostar with a mass of $1\ M_\odot$ and a temperature of 10°K, Eq. (2) gives a radius of 1.63×10^{17} cm (0.053 pc) and an initial density of 1.1×10^{-19} g cm^{-3} (4.8×10^4 atoms cm^{-3}), assuming that the gas constant $\mathcal{R}$ is equal to 3.36×10^7 erg g^{-1} °K^{-1} as would be the case for a composition of 65% molecular hydrogen, 32% helium, and 3% heavier elements (Gaustad 1963). For protostars with other masses and temperatures, the radius scales as M/T and the density scales as T^3/M^2, assuming that the Jeans criterion (2) is always satisfied.

If we assume that the temperature of a protostellar cloud is related to its density in the manner given by the third column of Table I, the Jeans mass M_J and the corresponding radius R_J can be calculated as a function of the initial density by making use of Eqs. (4) and (2). The resulting minimum unstable masses and radii are given in Table II, which also gives the corresponding visual optical depth at the center of the cloud. (These optical depths should be regarded as lower limits, since in general the protostar will be embedded in surrounding material which will provide additional shielding.) It is evident from Table II that the Jeans mass decreases rapidly with increasing density; in fact, the Jeans mass varies over almost the entire range of stellar masses as the density varies from 10^{-21} g cm^{-3} to 10^{-18} g cm^{-3}. Thus we expect that protostars can form by fragmentation at minimum densities in the range between about 10^{-21} g cm^{-3} and 10^{-18} g cm^{-3}, depending on the mass.

It is interesting to compare the predicted properties of protostars as listed in Table II with the observed properties of the 'Bok globules', certain small dense clouds which may represent protostars in an early stage of development

TABLE II

The Jeans mass and radius as functions of density

log ρ(g cm^{-3})	T(°K)	$M_J(M_\odot)$	$R_J(pc)$	τ
− 22	50.6	380.	3.9	0.30
− 21	25.4	43	0.88	0.68
− 20	15.6	6.5	0.22	1.7
− 19	8.4	0.81	0.051	3.9
− 18	5.1	0.12	0.013	10
− 17	5.4	0.042	0.0041	32

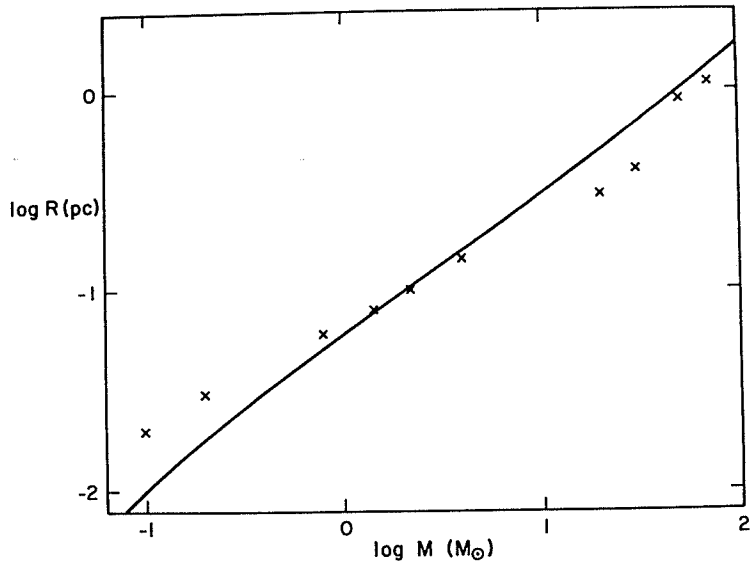

FIGURE 1 The crosses indicate the masses and radii of several dark globules as listed by Bok *et al.* (1971); for comparison the curve shows the theoretical mass-radius relation for protostars as given by Table II.

(Bok *et al.* 1971). The question of whether or not the Bok globules are protostars has been a controversial one; however, in a number of extended dark clouds such as those in Taurus one observes dense clumps or condensations which resemble some of the larger Bok globules, and star formation is almost certainly taking place in these dense condensations, as is suggested by the presence of large numbers of T Tauri stars. The classical Bok globules may represent some of the more isolated examples of such condensations. In Figure 1 the masses and radii of a number of typical globules, as estimated by Bok *et al.* (1971), are compared with the theoretical mass-radius relation for protostars as given by Table II. Considering that the estimated masses of the globules are probably uncertain by at least a factor of 2, the agreement between the properties of the globules and the predicted properties of protostars is striking and lends support to the possibility that at least some of the globules may be pre-stellar objects. Conversely, if it is accepted on other grounds that the globules are or resemble protostars, then the agreement with the theoretical predictions supports the assumption that the initial state of a protostar is given approximately by the Jean criterion.

5 THE COLLAPSE OF A SPHERICAL PROTOSTAR: ISOTHERMAL PHASE

We have seen that a protostar of moderate mass is expected to remain at an approximately constant temperature during the early optically thin stages of its collapse. Therefore it has usually been assumed in studying the early stages of the collapse of protostars that the collapse is isothermal. The mathematics is then simplified considerably, since the heating and cooling rates and the equation of conservation of energy need not be included explicitly. More detailed non-isothermal calculations have shown that small or moderate deviations from isothermality make no great difference to the development of a spherically collapsing cloud; therefore, in the next three sections we shall be concerned mainly with the results of isothermal collapse calculations.

For a system with spherical symmetry, the Eulerian equations of fluid dynamics with self gravitation can be written as follows:

$$\frac{\partial \rho}{\partial t} + \frac{1}{r^2}\frac{\partial}{\partial r}(r^2 \rho u) = 0 \tag{13}$$

$$\frac{\partial u}{\partial t} + u\frac{\partial u}{\partial r} + \frac{1}{\rho}\frac{\partial P}{\partial r} + \frac{Gm}{r^2} = 0 \tag{14}$$

$$\frac{\partial m}{\partial r} = 4\pi r^2 \rho \tag{15}$$

where u is the velocity in the radial (r) direction and m is the mass inside radius r. For an isothermal gas, the pressure P in Eq. (14) can be eliminated in favor of the density ρ by writing $P = \rho\mathcal{R}T$, where $\mathcal{R}T$ is a constant; the third term in Eq. (14) then becomes $\mathcal{R}Td \ln \rho/dr$. We then have a set of three partial differential equations for the three dependent variables ρ, u, and m as functions of the independent variables r and t.

The solution of Eqs. (13)–(15) is uniquely determined once the initial and boundary conditions for the collapsing cloud are specified. No analytical solution of these equations is known, but numerical solutions can be readily computed using a number of more or less standard numerical techniques for solving fluid dynamical problems with spherical symmetry. Such calculations have been made by several authors, each of whom has experimented with a number of different assumptions for the initial and boundary conditions (Penston 1966, Bodenheimer and Sweigart 1968, Larson 1969a, Appenzeller 1972). Despite the different methods of calculation and the different assumptions used, the results obtained are in all cases qualitatively very similar. The outstanding feature of the collapse which emerges from these calculations is that, contrary to some previous expectations, the collapse is always highly nonhomologous: even if the density of the cloud is initially uniform, the density distribution soon becomes strongly centrally condensed, and the degree of central condensation increases at an ever accelerating rate, leading to the runaway growth of a sharp central spike in the density distribution. As the collapse proceeds, the rapidly collapsing central core of the cloud shrinks in size and mass, and the bulk of the protostellar mass is 'left behind' in a more slowly collapsing extended envelope of infalling matter whose size and mean density are still much the same as those of the initial protostellar cloud. The growth of the central density peak continues unimpeded until the central density rises above 10^{-13} g cm^{-3} and the central part of the cloud becomes opaque to the infrared emission from the dust grains.

For a cloud whose density distribution is initially somewhat peaked at the center, the runaway growth of a sharp central density peak is readily understood from the fact that the free fall time

$$t_f = \left(\frac{3\pi}{32G\rho}\right)^{1/2} \tag{16}$$

is shortest at the point where the density is highest, i.e. at the center of the cloud, and therefore the central part of the cloud collapses most rapidly. As a result, the density contrast between the center and the outer part of the cloud is strongly amplified during the collapse. Even if the density distribution is initially uniform, an outward gradient of density and pressure is set up at the boundary of the cloud as soon as the collapse begins, and this

gradient begins to propagate inward at the speed of sound relative to the infalling material. In the language of classical gasdynamics (e.g. Zeldovich and Raizer 1968), a rarefaction wave is created at the surface of the cloud and begins to propagate inward at the speed of sound relative to the infalling material. The resulting outward pressure gradient causes the collapse to be decelerated from a free fall, first near the outer boundary and then progressively closer and closer to the center, so that the outer parts of the cloud collapse less rapidly than the central region and a centrally peaked density distribution is set up. A central 'plateau' remains in the density distribution until the rarefaction wave reaches the center, and the stage at which the plateau disappears depends on the ratio of the sound travel time to the free fall time (Bodenheimer and Sweigart 1968); however, if the initial conditions satisfy the Jeans criterion, the sound travel time is comparable with the collapse time, so that the rarefaction wave reaches the center and the central plateau disappears at an early stage in the collapse. From this point onward the density is no longer uniform anywhere but decreases monotonically outward from the center of the cloud, and the collapse continues nonhomologously as described above. The nonhomologous nature of the collapse cannot be avoided with any reasonable choice of boundary condition; in fact, the only situation in which homologous collapse can occur is in an infinite medium of strictly uniform density, which will maintain a uniform density as it collapses. However, this situation is clearly not relevant to star formation in our galaxy.

The development of the density distribution in an isothermally collapsing protostar is illustrated for a typical case in Figure 2, which shows the result for a protostar of mass $1 M_\odot$ and temperature 10°K which collapses from a uniform initial density of 1.1×10^{-19} g cm^{-3}, with a fixed boundary of radius 1.63×10^{17} cm. It is evident from the diagram that when the collapse gets well under way the major changes in density occur in a smaller and smaller region at the center and on a shorter and shorter time scale, while almost nothing happens in the outer part of the cloud, which still contains most of the mass. Note that the density distribution closely approaches the form $\rho \propto r^{-2}$, which is characteristic of all isothermal collapse calculations with spherical symmetry, regardless of the details of the initial and boundary conditions.

It is important that, while the time of collapse is approximately that of free fall, pressure gradient forces never become negligibly small but continue to play an important role in the dynamics of the collapse. This is because of the nonhomologous nature of the collapse and the resulting steep pressure gradients which are established within the collapsing cloud. Typically, pressure forces are found to be about half as large as gravity, and it is in fact the partial balance between pressure and gravity forces which is responsible for establishing the r^{-2} density law. The way in which this density law comes about can be understood as follows: Suppose that the initial

conditions satisfy the Jeans criterion, so that the rarefaction wave propagating inward from the boundary reaches the center at an early stage of the collapse; we then consider the later stages of the collapse when there no longer exists a central plateau of strictly uniform density. If we consider the part of the cloud within a very small radius r from the center (say, $r = 10^{15}$ cm), the density near the center is initially too low for this very small region to be gravitationally bound (or equivalently, for it to satisfy the Jeans criterion); the material in this region is confined by the pressure of the outer layers of the cloud rather than by its own gravity, and therefore its density remains nearly uniform as the collapse proceeds. As the density rises, however, a point is eventually reached where the mass within radius r becomes large enough that the Jeans criterion becomes satisfied in this region; the material in this region can then collapse gravitationally on its own without external compression, and the density distribution within radius r starts to become centrally condensed in the usual nonhomologous fashion. At the point when the Jeans criterion becomes satisfied for the region within radius r , the mass in this region is proportional to r (Eq. (2)), and the (still nearly uniform) density in this region is therefore proportional to r^{-2} . As the collapse proceeds, further changes in density occur mainly at radii smaller than r , so that the density at radius r remains proportional to r^{-2} . In this way a density law of the form $\rho \propto r^{-2}$ is progressively established at smaller and smaller radii.

It may be noted that what we have been discussing could be viewed as a fragmentation process, except that in a spherically symmetric cloud only one 'fragment' is formed, i.e. the central dense core of the cloud.

It can be demonstrated that in the isothermal case Eqs. (13)–(15) possess an asymptotic similarity solution, i.e. a solution in which the density and velocity distributions maintain the same form as the collapse progresses, and only the scale factors vary with time (Penston 1969a, Larson 1969a). It is evident from Figure 2 that the density distribution does show approximately this behavior, and although the density and velocity distributions do not agree exactly with the similarity solution of Penston (1969a) and Larson (1969a) they appear to approach the similarity solution asymptotically as the collapse progresses. Thus the similarity solution can serve as a useful semi-analytic limiting form for the density and velocity distributions produced during the collapse of an isothermal sphere. We shall therefore summarize some properties of the asymptotic similarity solution which may be of interest:

1) At large distances from the center, the density and velocity distributions approach the asymptotic forms

$$\rho = 0.705 \frac{\mathcal{R}T}{G} r^{-2} \qquad (17)$$

$$u = 3.28 (\mathcal{R}T)^{1/2} . \qquad (18)$$

These relations also give the limiting values of ρ and u which are attained at any fixed radius r as the central density increases indefinitely. Note that the collapse velocity during the isothermal phase of the collapse never exceeds 3.28 times the isothermal sound speed; for a temperature of 10°K, this means that the maximum collapse velocity attained during the isothermal phase of the collapse is 0.6 km s^{-1} .

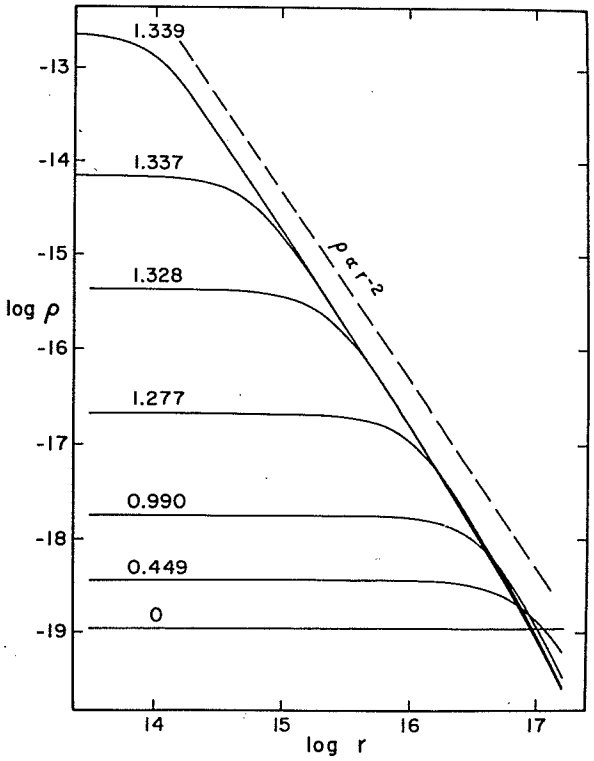

FIGURE 2 The density distribution at several times during the isothermal collapse of a protostar with a mass of $1\ M_\odot$, a radius of 1.63×10^{17} cm , and a temperature of 10°K. The numbers marked on the curves give the time elapsed in units of 10^{13} s. (From Larson 1969a).

2) At the center of the cloud the ratio of pressure to gravity forces is 0.60, so that the acceleration of the collapse is reduced to 0.40 times the free fall acceleration and the collapse time scale is increased by a factor of $(0.40)^{-1/2} = 1.58$ relative to the free fall time. At large distances from the center, the ratio of pressure to gravity forces drops to a limiting value of 0.23.

3) The asymptotic similarity solution depends only on the isothermal sound speed $(\mathcal{R}T)^{1/2}$ and is independent of the initial and boundary conditions for the collapsing cloud; for example, it is independent of such quantities as the mass and the radius of the cloud. Thus, as long as the temperature remains isothermal and is the same in all cases, the behavior of the inner part of a collapsing cloud is independent of the total mass or size of the cloud.

6 THE COLLAPSE OF AN AXISYMMETRIC NON-ROTATING CLOUD

Since there is no *a priori* reason why a collapsing cloud should begin with a spherical shape or maintain spherical symmetry as it collapses, it is necessary before one can have a complete understanding of the dynamics of collapsing clouds to investigate the effect of deviations from spherical symmetry on the collapse. At present the only available non-spherical collapse calculations refer to the case of a cloud with axial symmetry (Larson 1972a). The restrictionsto axial symmetry still allows one to study the important special cases of clouds with prolate or oblate shapes. It is known that in the absence of pressure forces, an oblate spheroid will collapse to a disc, whereas a prolate spheroid will collapse to a line (Lin, Mestel, and Shu 1965); clearly, it is important to establish whether the same type of behavior occurs in a more realistic fluid dynamical calculation in which pressure forces are included.

Another important problem which can be studied under the assumption of axial symmetry is the collapse of a rotating cloud, at least as long as deviations from axial symmetry do not become important. This problem will be discussed in the following section, but in order to avoid repeating equations which are nearly identical we shall include the rotation terms in the equations for the collapse of an axisymmetric cloud which are given below.

In terms of the spherical polar coordinates r, θ, ϕ, and the corresponding velocity components u, v, w, the Eulerian fluid dynamical equations for a system with axial symmetry can be written as follows, where Φ denotes the gravitational potential:

$$\frac{\partial \rho}{\partial t} + \frac{1}{r^2}\frac{\partial}{\partial r}(r^2 \rho u) + \frac{1}{r \sin\theta}\frac{\partial}{\partial \theta}(\sin\theta\, \rho v) = 0 \qquad (19)$$

$$\frac{\partial u}{\partial t} + u\frac{\partial u}{\partial r} + \frac{v}{r}\frac{\partial u}{\partial \theta} + \frac{1}{\rho}\frac{\partial P}{\partial r} + \frac{\partial \Phi}{\partial r} - \frac{v^2 + w^2}{r} = 0 \qquad (20)$$

$$\frac{\partial v}{\partial t} + \frac{u}{r}\frac{\partial}{\partial r}(rv) + \frac{v}{r}\frac{\partial v}{\partial \theta} + \frac{1}{\rho r}\frac{\partial P}{\partial \theta} + \frac{1}{r}\frac{\partial \Phi}{\partial \theta} - \frac{w^2}{r \tan\theta} = 0 \qquad (21)$$

$$\frac{\partial w}{\partial t} + \frac{u}{r}\frac{\partial}{\partial r}(rw) + \frac{v}{r \sin\theta}\frac{\partial}{\partial \theta}(\sin\theta\, w) = 0 . \qquad (22)$$

In order to calculate the gravitational potential Φ these equations must be supplemented with the Poisson equation:

$$\nabla^2 \Phi = \frac{1}{r^2}\frac{\partial}{\partial r}\left(r^2 \frac{\partial \Phi}{\partial r}\right) + \frac{1}{r \sin\theta}\frac{\partial}{\partial \theta}\left(\sin\theta \frac{1}{r}\frac{\partial \Phi}{\partial \theta}\right) = 4\pi G\rho . \qquad (23)$$

As before, we can assume that during the early stages of the collapse the cloud remains isothermal, so that the equation of conservation of energy need not be included explicitly and the pressure P in Eqs. (20) and (21) can be evaluated from $P = \rho \mathcal{R}T$ where $\mathcal{R}T$ is a known constant. In writing Eq. (22) we have assumed that no torques act on the cloud and that the angular momentum of each fluid element is conserved during the collapse. In the present section we shall consider only the case of a non-rotating cloud, i.e. $w = 0$.

Numerical solutions of Eqs. (19)–(23) have been computed by Larson (1972a) for a number of choices of initial conditions. These calculations employed a fixed spherical boundary, as in many of the spherically symmetric collapse calculations, but the density distribution within the boundary was allowed to be either elongated (prolate) or flattened (oblate). The results of these calculations showed that if the initial conditions are approximately consistent with the Jeans criterion, then small deviations from spherical symmetry are not amplified during the collapse, contrary to the results for the pressure free case; instead, small deviations from spherical symmetry tend to oscillate between prolate and oblate forms as the collapse proceeds. Apart from these small oscillatory deviations from spherical symmetry, the collapse proceeds just as in the spherical case with the runaway growth of a central spike in the density distribution. Thus it is clear that in these calculations the pressure forces, while not sufficient to halt the collapse, are nevertheless sufficient to maintain approximate spherical symmetry as the cloud collapses.

When large initial deviations from spherical symmetry were assumed, the calculations again showed that pressure forces, if important initially, tend to produce an approach to spherical symmetry or at least to prevent the growth of large deviations from spherical symmetry. A typical result is illustrated in Figure 3; here the initial density distribution is elongated vertically and the iso-density contours are vertical cylinders (Figure 3(a)). After the cloud has collapsed significantly, it becomes strongly centrally condensed and the density contours in the rapidly collapsing central part of the cloud become nearly spherical (Figure 3(b)). Although the calculations were not carried very far

beyond this point, it seems likely that the collapse would continue very much as in the spherical case. Similar results are found in the case of an initially flattened density distribution if pressure forces are important initially. It is noteworthy that in both cases all of the material in the cloud collapses into a single central condensation; the cloud shows no tendency to develop more than one center of condensation, i.e. no tendency to fragment.

If the initial ratio of pressure to gravitational forces is smaller than in the cases discussed above, appreciable deviations from spherical symmetry may persist or even grow during the collapse. Here it is important to distinguish between a flattened and an elongated density distribution. In the case of an initially flattened density distribution, the density contours can retain an appreciable degree of flattening as the cloud collapses and condenses centrally, but the degree of flattening remains approximately constant and does not increase indefinitely as the collapse proceeds. The more interesting case is that of an elongated cloud; in this case, the behavior of the cloud is found to depend on whether the mass per unit length is larger or smaller than a critical value

$$\frac{M}{L} = \frac{2\mathcal{R}T}{G} \tag{24}$$

appropriate for an equilibrium isothermal cylinder (Ostriker 1964). If M/L is smaller than the critical value (24), the cylinder expands laterally and the density distribution becomes more nearly spherical, as in Figure 3(b). If M/L exceeds the critical value (24) the cylinder collapses toward its axis and becomes a thin filament, as expected from the discussions of McCrea (1957) and Mestel (1965a). An example of this is illustrated in Figure 4, which shows the result obtained when the same initial configuration as in Figure 3(a) is assumed but the (constant) temperature is reduced from 10°K to 7.5°K, thus making the right hand side of Eq. (24) ($\sim 7.4 \times 10^{15}$ g cm^{-1}) smaller than the left hand side ($\sim 1.0 \times 10^{16}$ g cm^{-1}). It is evident in Figure 4 that, while collapsing toward its axis, the cloud has also begun to fragment, i.e. to develop two centers of condensation somewhat removed from the center of the cloud along the vertical axis. The result that an elongated cloud collapsing toward its axis tends to fragment into subcondensations along its length is not surprising in view of the fact that the Jeans criterion indicates that a cylinder which is unstable to collapse toward its axis is also unstable to longitudinal fragmentation on scales comparable to or greater than the thickness of the cylinder (Mestel 1965a).

Thus from the available non-spherical collapse calculations it appears that in most cases, if the initial conditions approximately satisfy the Jeans criterion, pressure forces will tend to maintain rough spherical symmetry during the collapse of an isothermal non-rotating cloud and thus prevent fragmentation.

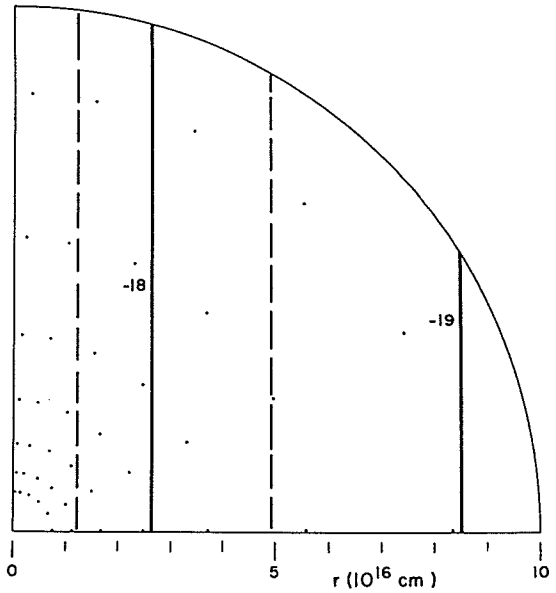

FIGURE 3(a) The initial density distribution assumed in calculating the collapse of an axisymmetric cloud with an elongated density distribution. The vertical axis is the axis of symmetry, and only one quadrant of the meridional plane is shown. The solid lines are the isodensity contours corresponding to integral values of log ρ, as marked, and the dashed lines are for half-integral values. The dots represent the grid points at which the densities are calculated.

The principal exception to this is the case of an elongated cloud whose mass per unit length exceeds the critical value (24); in this case the cloud collapses toward a thin filament, but at the same time the filament tends to fragment into subcondensations along its length. These results suggest that the only type of deviation from spherical symmetry which is likely to be amplified by gravitational collapse is an elongated or filamentary structure, and that if a cloud does not collapse roughly spherically it will tend to collapse to a filament which then fragments into subcondensations along its length. This prediction may be relevant in connection with certain filamentary dark clouds such as those in Taurus, which contain conspicuous knots or condensations along their length. In addition, the existence of chains of galaxies is suggestive that the intergalactic gas may in some cases have condensed into filaments which then fragmented into galaxies.

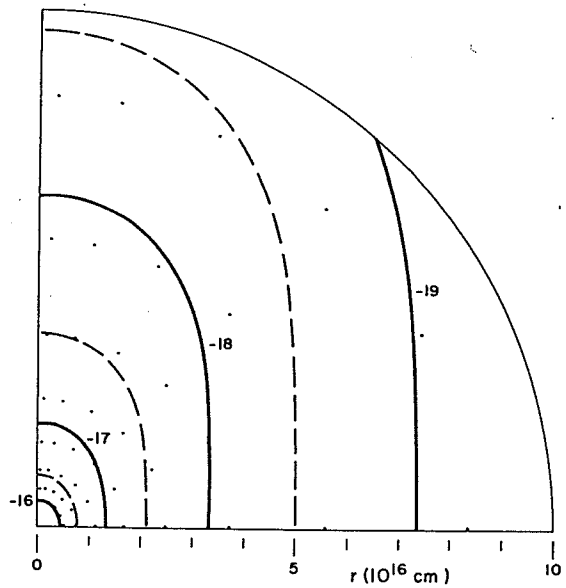

FIGURE 3(b) The density distribution resulting from the collapse of the configuration illustrated in Figure 3(a) when a constant temperature of 10°K is assumed. (From Larson 1972a.)

7 THE COLLAPSE OF AN AXISYMMETRIC ROTATING CLOUD

In general, a collapsing protostellar cloud will probably have a significant amount of angular momentum, and if this angular momentum is conserved during the collapse, it will have an important effect on the dynamics of the collapse. In particular, it is clear that in the presence of a finite angular momentum the material of the cloud cannot all fall into the center. The only available collapse calculations for rotating clouds (Larson 1972a) are rather crude, but they suffice to illustrate some of the important possible effects of rotation on the collapse.

If a cloud is rotating rapidly enough, its rotation can help to stabilize the cloud against gravitational collapse. The Jeans criterion must therefore be modified for a rapidly rotating cloud. Some trial collapse calculations have been made for cases in which both pressure and centrifugal forces are important (Larson 1972a); in these calculations it has been assumed that the cloud begins with uniform density and uniform rotation and collapses within a fixed spherical boundary, as before. With these assumptions, it is found that collapse will occur if the following approximate criterion is satisfied:

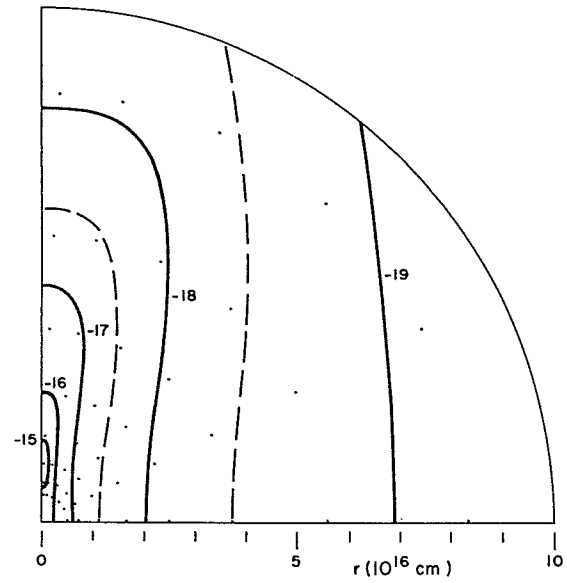

FIGURE 4 The density distribution resulting from the collapse of the configuration illustrated in Figure 3(a) when a constant temperature of 7.5°K is assumed. (From Larson 1972a.)

$$E_R \lesssim 0.42 \frac{GM}{R} - \mathcal{R}T$$

or

$$R \lesssim 0.42 \frac{GM}{\mathcal{R}T + E_R} \qquad (25)$$

where

$$E_R = \frac{1}{5}\omega^2 R^2$$

is the rotational kinetic energy per unit mass. This criterion indicates, as would be expected, that if a cloud is rotating ($E_R > 0$) it must be more compressed (i.e., must have a smaller radius) than a nonrotating cloud if gravity is to overcome the combined effects of pressure and centrifugal forces and cause the cloud to collapse.

If criterion (25) is safely satisfied and centrifugal force is initially less important than gravity, the cloud begins to collapse in the same nonhomologous fashion as was found for a non-rotating cloud: the central part of the cloud collapses most rapidly, and the density distribution soon becomes

peaked at the center. If the angular momentum of each fluid element is conserved, as assumed in the calculations of Larson (1972a), the ratio of centrifugal to gravitational forces increases as the collapse proceeds. Since the collapse proceeds most rapidly at the center, it is in the dense central 'core' of the cloud that the centrifugal force first becomes large enough to balance or overbalance gravity and halt further collapse toward the axis of rotation. Meanwhile, in the outer part of the cloud centrifugal force has not yet become large enough to balance gravity, and the material continues to fall inward and accumulate in a ring-shaped region around the periphery of the central region which has stopped collapsing. As a result, the density in this ring-shaped region rises more rapidly than the central density, and soon exceeds the central density. Gravity then tends to pull more material into the ring-shaped region of maximum density, and a doughnut-like configuration with a central density minimum begins to form in the inner part of the cloud. A typical result is illustrated in Figures 5(a) and 5(b); Figure 5(a) shows the density contours in the outer part of the cloud, and Figure 5(b) is an enlargement of the central part of Figure 5(a) showing clearly the ring-shaped region of maximum density, which has a radius of about 5% of the radius of the cloud and contains about 20% of the total mass.

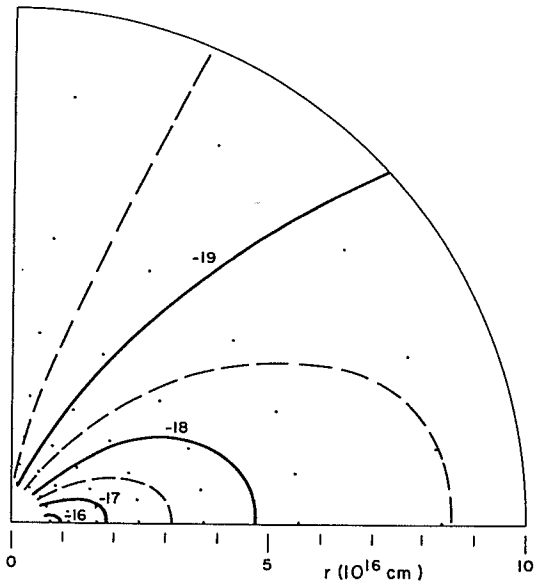

FIGURE 5(a) The density distribution resulting from the collapse of an initially uniform and uniformly rotating cloud of mass $1\ M_\odot$, initial density 4.8×10^{-19} g cm^{-3}, and initial initial angular velocity 3×10^{-13} s^{-1}. The vertical axis is the axis of rotation.

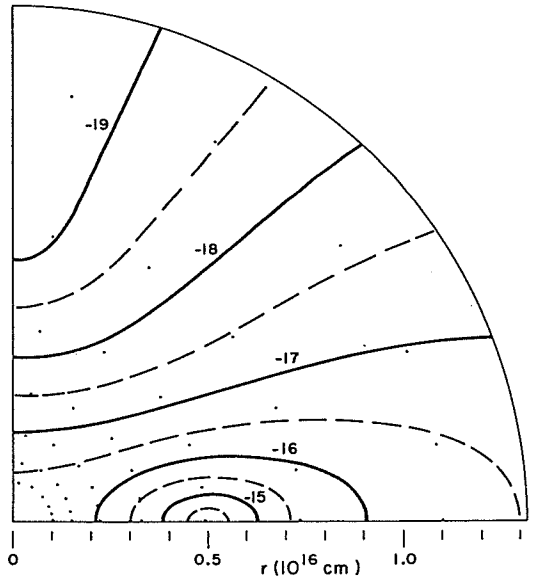

FIGURE 5(b) An enlargement of the central part of Figure 5(a) to show more clearly the ring-shaped region of maximum density which forms near the center of the cloud. (From Larson 1972a.)

A rapidly rotating doughnut-like configuration such as that shown in Figure 5(b), whose maximum density occurs away from the axis of rotation, is almost certainly unstable to non-axisymmetric perturbations and will presumably fragment into two or more subcondensations orbiting about the center of the cloud. This is suggested by the stability criterion of Ostriker and Bodenheimer (1973), according to which a rotating fluid configuration is unstable to non-axisymmetric modes if the ratio of rotational kinetic energy to gravitational binding energy exceeds about 0.26; for comparison, the value of this ratio for the configuration shown in Figure 5(b) is approximately 0.4, well above the critical value for instability. In fact, it is likely that non-axisymmetric deformations will become important even before a well defined ring-shaped configuration has formed in the central part of the cloud; this is suggested by the fact that the available stability analyses for rotating fluid configurations (e.g. Bardeen 1971) show that the non-axisymmetric modes always become unstable before the ring modes. A sufficiently rapidly rotating cloud might then fragment directly into two or more condensations orbiting around each other, without ever forming a ring.

Evidently a full three-dimensional calculation will be required to follow the collapse of a rotating cloud beyond the point where deviations from axial symmetry become important, and since such calculations are not yet available, the later development can only be conjectured. If the cloud fragments into

subcondensations, as seems likely, the subcondensations will in general have an appreciable amount of intrinsic or spin angular momentum; this follows from Kelvin's circulation theorem, which states that the vorticity of any fluid element must increase as it is compressed (provided that magnetic or viscous torques do not act). Consequently, the subcondensations may undergo further stages of rotational fragmentation as they continue to collapse to higher densities. The tendency toward further fragmentation will be counteracted by tidal interactions between neighboring subcondensations, which will tend to slow down their rotational motions and transfer angular momentum from spin to orbital form, thus facilitating further collapse of the subcondensations and making their fragmentation less likely. Thus without detailed calculations it is difficult to say just how much fragmentation is likely to occur. In any case, it appears probable that the end result of the collapse of a rotating cloud will be the formation of some sort of multiple system of stars orbiting around each other. This would then account naturally for the prevalence of binary and multiple systems in the sky, and even the single stars might be plausibly accounted for as escapers from small multiple systems which have disintegrated (Larson 1972a).

If we confine attention to the formation of a single star in one of the subcondensations that form in a rotating cloud, this will probably have some basic similarities to the formation of a star in a non-rotating cloud. This is suggested by the fact that all of the available collapse calculations, including those which incorporate rotation, show a very non-homologous behavior characterized by the development of small regions of much higher than average density which then act as centers of condensation for the remaining material. In the spherical, non-rotating case a small stellar core or 'embryo star' first forms at the center of the cloud and then grows into a pre-main sequence star of normal mass by accretion of part or all of the remaining uncondensed material in the cloud (Sections 9–13). A similar process may occur even in a more general situation, for example in a subcondensation in a rotating cloud, the principal difference being that more than one embryo star may form in a single cloud or condensation. The results to be described in Sections 9–13 for the collapse of a spherical, non-rotating protostar may then have a more general relevance, at least as far as the basic qualitative features are concerned. The relevance of the spherical collapse calculations to more general circumstances is also supported by the generally good agreement between the predicted and observed properties of protostars and young stars (Larson 1972b). Consequently we shall in the rest of this article confine attention primarily to the case of a spherical, non-rotating protostar.

8 COMMENTS ON MAGNETIC FIELDS

It has long been realized that magnetic fields, like rotation, can play an important role in the dynamics of collapsing interstellar clouds. A number of authors have discussed the effect of a magnetic field on the collapse of a gas cloud, generally within the context of simplified models in which it is assumed, for example, that the collapsing cloud maintains uniform density (Mestel 1956b, Spitzer 1968a, b). However, such simplifying assumptions may not be very closely realized in practice, in which case it is difficult to draw many quantitative conclusions about the effect of a magnetic field on a collapsing cloud. It will be necessary for this purpose to carry out detailed dynamical collapse calculations incorporating magnetohydrodynamic effects, but as yet no such calculations are available.

One of the major problems in estimating the importance of magnetic fields in collapsing clouds concerns the degree of coupling between the magnetic field and the gas; this depends critically on the degree of ionization, which in turn depends on the detailed processes responsible for ionization and recombination. It is thought that ionization may be produced mainly by cosmic rays, whereas recombination may occur primarily on the surfaces of dust grains (Spitzer 1968b). Both ionization and recombination rates are uncertain, the former because it depends on the opacity of the cloud to low energy cosmic rays, and the latter because it depends on the properties of the dust grains. Spitzer (1968b) has estimated that during the early stages of the collapse of an interstellar cloud the time required for a magnetic field to diffuse out of the cloud will exceed the free fall time, so that the magnetic field remains closely coupled to the gas (frozen in) and is compressed as the cloud collapses. However, in some dense cold clouds the measured magnetic field is much weaker than would be predicted if the magnetic field had remained frozen into the cloud after its formation (Verschuur 1971). This suggests that in at least some cases the magnetic field may be able to escape from the cloud at an early stage of the collapse and may play a less important role than anticipated for the dynamics.

Even if the magnetic field remains frozen into the gas during the early stages of the collapse, the cloud will eventually become so dense that cosmic rays are completely shielded out and the degree of ionization drops to an extremely low value, allowing the magnetic field to escape from the cloud. For a cloud of mass $10^4\ M_\odot$ this occurs at a density of the order of 10^{-15} g cm^{-3} (Nakamo and Tademaru 1972). Up to this point the magnetic field may inhibit the formation of small condensations in the collapsing cloud, but at higher densities collapse and fragmentation can proceed freely, unimpeded by magnetic fields. Thus the principal effect of a magnetic field may be to inhibit fragmentation and to increase the effective initial density from which a protostar can begin to collapse freely, but the later stages of the collapse

process should not be much affected by magnetic fields. As will be seen, an increase in the initial density by a few orders of magnitude does not alter the basic qualitative features of the collapse, but can result in some significant quantitative differences in the properties of the resulting star.

9 THE COLLAPSE OF A SPHERICAL PROTOSTAR: NON-ISOTHERMAL STAGES

We proceed now to consider the further evolution of a spherically collapsing protostar following the initial isothermal phase described in Section 5. Calculations of the later non-isothermal stages of the collapse have been carried out by Larson (1969a, 1972b) and Appenzeller (1972).

When the central density in a collapsing protostar reaches a value of the order of 10^{-13} g cm^{-3}, the central part of the cloud starts to become opaque to the infrared radiation from the dust grains; the thermal energy generated by the collapse is then no longer freely radiated away and the central temperature begins to rise significantly above its initial value of $\sim 10^{\circ}$K. The assumption of isothermality can then no longer be used, and it becomes essential to incorporate the equation of conservation of energy (i.e., the first law of thermodynamics) into the fluid dynamical equations and to treat explicitly the transfer of energy by the infrared radiation from the dust grains.

In Eulerian form the equation of conservation of energy for a system with spherical symmetry can be written

$$\frac{\partial E}{\partial t} + P \frac{\partial}{\partial t} \frac{1}{\rho} + u \left(\frac{\partial E}{\partial r} + P \frac{\partial}{\partial r} \frac{1}{\rho} \right) + \frac{3}{4\pi r^2 \rho} \frac{\partial L}{\partial r} = 0 \qquad (26)$$

where $E(r, t)$ is the specific internal energy of the gas and $L(r)$ is the rate at which energy is transported by radiation or convection across a surface of radius r. During the early stages of the evolution of a protostar, convective instability does not arise and energy is transported only by radiation; the energy flux $L(r)$ is then given by the solution of a radiative transfer problem, which in general is quite complicated because of the spherical geometry and because of the large range of optical depths which must be considered. For large optical depths, however, the radiative transfer problem simplifies greatly and we can use the radiative diffusion equation as used in the theory of stellar interiors; this equation can be written

$$L = -\frac{64 \pi \sigma r^2 T^3}{3 \kappa \rho} \frac{dT}{dr} . \qquad (27)$$

The evolution of the opaque central region of the collapsing protostar can then be computed by using Eqs. (13), (14), (15), (26), and (27) together with an equation of state specifying P and E as functions of ρ and T.

While Eq. (27) is strictly applicable only in optically thick regions, it happens that when it is applied in an optically thin region it has the effect of artificially forcing the temperature to be constant and equal to the boundary temperature. Since the outer optically thin part of the protostar is expected to be nearly isothermal anyway, Eq. (27) can in fact be applied throughout the cloud and will yield approximately the correct temperatures in both the optically thick and the optically thin regions if a boundary temperature of $\sim 10^{\circ}$K is specified. This fortunate situation does not hold during the later stages of the collapse when the luminosity from the hot central core of the protostar begins to heat up the outer optically thin layers. A better approximation for calculating the temperature distribution throughout the cloud in these circumstances will be described in Section 11.

In using Eq. (27) to calculate the radiative energy flux, it is necessary to know the Rosseland mean opacity κ of the protostellar material. For the temperature range below about 1500–2000°K in which dust grains can exist, the dust grains constitute by far the most important source of opacity. Data for the Rosseland mean opacities produced by dust grains of various compositions have been given by Gaustad (1963) and by Kellman and Gaustad (1969); however, because the composition and the structure of the dust grains are still not well determined, the Rosseland mean opacity of the protostellar material at the relevant low temperatures remains rather uncertain. The collapse calculations of Larson (1969a, 1972b) have adopted a simple constant value of 0.15 cm^{2}g^{-1} for the Rosseland mean opacity of the dust grains; this was intended to represent a rough mean value of the available data over the relevant temperature range. Fortunately, trial calculations made with different opacities have shown that for a protostar of mass near $1\ M_{\odot}$ the principal results of the collapse calculations are rather insensitive to the assumed infrared opacity of the dust grains. (For massive protostars this conclusion may require modification, since in this case the effect of radiation pressure on the dust grains may be important for the dynamics of the collapse; see Sections 13 and 14.)

As we have noted, when the central density rises above $\sim 10^{-13}$ g cm^{-3} the central dense core of the cloud starts to become opaque, and radiative energy losses from this region soon become relatively unimportant; the further collapse of the core of the cloud then becomes nearly adiabatic rather than isothermal, and the central temperature and pressure begin to rise rapidly. By the time the central density has reached $\sim 10^{-12}$ g cm^{-3}, the rising pressure has begun to decelerate the collapse at the center, and by the time the central density has reached $\sim 10^{-10}$ g cm^{-3} and the central temperature has risen to a value somewhat over 100°K, the collapse has been

practically brought to a halt within the opaque core of the cloud.

Because of the non-homologous nature of the collapse, the opaque core contains only a very small fraction ($\approx 1\%$) of the total mass of the cloud; most of the mass remains in the outer part of the cloud which is still optically thin and still continuing to fall inward almost in free fall. Thus at the boundary of the opaque core there arises a steep velocity gradient between the inner region where the collapse has almost been stopped and the outside region where the material continues to fall in freely; this velocity gradient quickly steepens into a shock front in which the infalling material is suddenly stopped as it strikes the surface of the core.

When the collapse of the opaque core is first halted by pressure gradients, there is a small rebound amounting to about 20 percent in radius, followed by a series of radial oscillations of the core about a hydrostatic equilibrium configuration. The initial mass and radius of the core are approximately $6 \times 10^{-3}\ M_\odot$ and 5 AU respectively, and its central density and temperature are about 3×10^{-10} g cm^{-3} and 200°K respectively; these numbers are rather uncertain owing to the difficulty in defining precisely the instant at which the core forms. The initial properties of the opaque core depend on the temperature and opacity of the material in the collapsing protostellar cloud, but not on the total mass of the cloud, as long as the initial conditions approximately satisfy the Jeans criterion; this is because during the isothermal phase of the collapse the density and velocity distributions in the inner part of the cloud approach the asymptotic similarity solution described in Section 5, which depends only on the temperature and not on the total mass of the cloud.

As material continues to fall into the core, the core grows in mass but shrinks in radius because the outer part of the core continues to lose energy through radiative energy transfer, even though the optical depths are large. Meanwhile the central part of the core remains nearly adiabatic, and the central density and temperature rise rapidly as the core grows in mass and shrinks in size. After about 300 years the core attains a mass of about $1.1 \times 10^{-2}\ M_\odot$ and a radius of about 1.7 AU ; at this point the central density and temperature are about 10^{-7} g cm^{-3} and 1900°K respectively, and the hydrogen molecules at the center of the core are beginning to dissociate. This reduces the ratio of specific heats γ below the critical value 4/3 and triggers a second phase of dynamical collapse near the center of the core. Since most of the internal energy generated by the collapse goes into dissociating the hydrogen molecules rather than into thermal motions, the temperature rises only slowly with increasing density. The central collapse of the core therefore resembles the initial isothermal collapse of the whole cloud, and again leads to non-homologous development of a sharp central peak in the density distribution. The dynamical collapse of the central part of the opaque core continues through several orders of magnitude in density until nearly all of the hydrogen molecules

have been dissociated and γ again rises above 4/3. The central temperature and pressure than begin to rise sufficiently rapidly to once again halt the collapse and cause the formation of a second hydrostatic core at the center of the first core, part of which is now falling inward almost in free fall. The outer layers of the first core and the shock front bounding it have not changed significantly during the short time interval ($\sim$ 1 year) since the beginning of the second central collapse, but the material of the first core continues to fall inward and accrete on the second core, and after a further $\sim$ 10 years all traces of the first core and of the shock front bounding it have disappeared.

When the second core first forms, it has a mass of $\sim 1.5 \times 10^{-3}\ M_\odot$, a radius of $\sim 1.2\ R_\odot$, a central density of $\sim 2 \times 10^{-2}$ g cm^{-3} , and a central temperature of $\sim 2 \times 10^4$ °K . Again, these numbers are difficult to define precisely and they depend somewhat on the temperature and opacity of the initial protostellar cloud, but they do not depend on the total mass of the cloud or on the precise initial conditions for the collapse. The second core, like the first, is bounded by a shock front in which the material falling into the core is suddenly brought to rest. It is noteworthy that, apart from its initially very small mass of $\approx 10^{-3}\ M_\odot$, the second core has properties much like those of an ordinary star; we shall therefore refer to it as a 'stellar core'.

The time elapsed from the beginning of the collapse to the formation of the stellar core is approximately equal to the free fall time for the initial cloud. If the cloud begins at rest with a radius given by Eq. (2), the collapse time is about 1.5 free fall times, or about 3×10^5 years for a protostar of one solar mass with an initial temperature of 10°K. At the time of formation of the stellar core, the bulk of the mass of the protostar still remains distributed in the outer part of the cloud and has not fallen inward very far since the beginning of the collapse because of the retarding effect of pressure gradients in the outer part of the cloud. The infall of the outer layers of the protostar requires a few additional free fall times for its completion, and the infall of these outer layers into the already formed stellar core is the dominant process of the later evolution of the protostar. The stellar core continues to grow in mass at the expense of the rest of the cloud, and it eventually acquires the bulk of the protostellar mass. After all of the original material has either been accreted on the core or dissipated in some other way (e.g., by radiation pressure), the stellar core emerges from its surrounding envelope as a newborn pre-main sequence star.

In following these later stages of evolution of a protostar, it is necessary to compute in some detail the evolution of the central stellar core or 'embryo star'. The evolution of this embryo star is governed primarily by the rate at which material falls into it and by the properties of the shock front at its surface through which the infalling matter passes. This is particularly true of protostars with masses less than $\sim 3\ M_\odot$, for which radiative energy transport within the core is unimportant and the core material behaves isentropically,

conserving the entropy which it acquired on passing through the shock front. It is therefore essential to consider in some detail the properties of the shock front and to incorporate an adequate treatment of the shock front in the evolutionary calculations. Accordingly we discuss in the following section the treatment of the accretion shock.

10 TREATMENT OF THE ACCRETION SHOCK

In ordinary adiabatic gas dynamics, shock fronts are generally thin enough to be treated as discontinuities in the flow. One can then derive a set of 'shock jump conditions' relating the values of the flow variables on the two sides of the discontinuity, assuming that mass, momentum, and energy are conserved in the flow across the shock front. In the present situation, however, the temperature in the accretion shock becomes so high that radiative energy losses become important; in this case the shock front is followed by a region of radiative cooling in which the temperature decreases and the density rises, both variables eventually approaching limiting values at large optical depths inside the shock front. Since the thickness of the radiative cooling region inside the shock front is small compared with the dimensions of the stellar core, it is still adequate as far as the large scale dynamics is concerned to treat the whole shock region, including the cooling region, as a discontinuity in the flow. However, one can no longer assume conservation of energy in the shock region without taking the radiative energy losses into account. In order to determine the structure of the shock region and the limiting values of the temperature and density inside the shock front, it is therefore necessary to solve a radiative transfer problem in conjunction with the dynamics. Since a detailed solution of this problem is not yet available, we shall describe a simple approximation which involves treating the shock region as a discontinuity and deriving analogues of the classical shock jump conditions relating the values of the flow variables at two suitably chosen surfaces just inside and outside the shock front.

The temperature profile expected in the vicinity of the shock front is sketched schematically in Figure 6. The shock front is located at $r = R$ and is represented by the large discontinuous jump in temperature, followed by a rapid drop in temperature due to radiative cooling. The temperature levels off inside the shock front as large optical depths are approached, but it eventually begins to rise again in the deep interior of the core. Outside the shock front the infalling material absorbs some of the radiation from the hot region inside the shock front, causing its temperature to rise as it approaches the shock. In Figure 6 the surfaces $r = r_1$ and $r = r_2$ represent two suitable bounding surfaces of the shock region which are chosen such that most of the rapid temperature variations connected with the shock front occur between r_1 and

r_2 but the shock thickness $|r_2 - r_1|$ is still small compared with the core radius R.

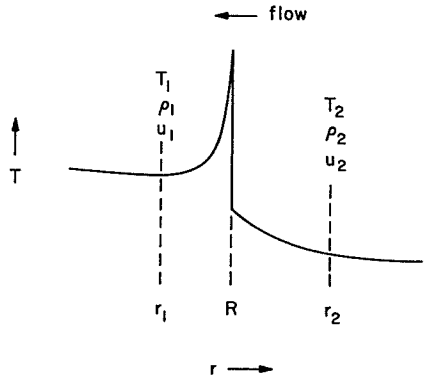

FIGURE 6 A schematic illustration of the temperature distribution in the vicinity of the accretion shock at $r = R$.

We now consider the problem of deriving analogues of the classical shock jump conditions relating the values of the flow variables at r_1 and r_2. This may be done by considering the conservation of mass, momentum, and energy in the shock region between r_1 and r_2, taking into account the gravitational force acting on this region and the radiative energy flux through it. Since the velocity with which the shock front moves is much smaller than the infall velocity, we can with good accuracy assume that the shock front is stationary and use a fixed frame of reference. The equation of conservation of mass, obtained by equating the mass flux at r_1 to that at r_2, is then

$$\rho_1 u_1 = \rho_2 u_2 \tag{28}$$

where the subscripts 1 and 2 denote quantities evaluated at r_1 and r_2, respectively.

To derive the momentum conservation relation, we assume that the rate at which momentum is added to the material passing through the shock region is equal to the net force exerted on this region by pressure and gravity forces. The momentum flux into the shock region at r_2 is equal to $\rho_2 u_2^2$ and the outward momentum flux at r_1 is $\rho_1 u_1^2$, so that the rate at which inward momentum is added to the material passing through the shock region is $\rho_1 u_1^2 - \rho_2 u_2^2$. The net inward pressure force acting on this region is $P_2 - P_1$, and the gravitational force per unit area is

$$g \int_{r_1}^{r_2} \rho \, dr$$

where $g = GM/R^2$ is the gravitational acceleration at the surface of the core and M and R are the mass and radius of the core. We then have, equating the rate of momentum change to the force acting per unit area,

$$\rho_1 u_1^2 - \rho_2 u_2^2 = P_2 - P_1 + g \int_{r_1}^{r_2} \rho \, dr . \tag{29}$$

(This equation can also be derived by integrating the momentum Eq. (14) between r_1 and r_2, neglecting the time derivatives and assuming a steady flow.)

During most of the evolution of a protostar the last term in Eq. (29) is unimportant, and the equation reduces to the standard momentum equation for a thin shock front. During the final stages of the infall process, however, the quantities ρ_2, P_2, and u_1 all become very small and the pressure P_1 at the surface of the core is determined, as in a normal stellar atmosphere, by the weight of the layers above r_1. In these circumstances it is convenient to follow the usual practice for stellar models and take the surface $r = r_1$ to be the photosphere of the stellar core, i.e. the surface at which the local temperature T_1 is equal to the effective temperature T_e; according to the Eddington approximation this occurs at an optical depth of 2/3. The last term in Eq. (29) can be re-expressed as an integral over optical depth if we make the substitution $g\rho dr = -(g/\kappa)\, d\tau$; we then need the integral of this quantity from optical depth $\tau = 0$ to $\tau = 2/3$. To obtain an approximation to this integral, we assume that its value is the same as that which it would have in a normal hydrostatic stellar atmosphere; we can then use the standard equilibrium relation for a hydrostatic atmosphere:

$$dP = \frac{g}{\kappa} \, d\tau \tag{30}$$

(which also follows from Eq. (29) if the dynamical pressure ρu^2 is neglected). Assuming an isothermal atmosphere we have, roughly, $\kappa \propto \rho^{1/2} \propto P^{1/2}$; substituting $\kappa = \kappa_0 P^{1/2}$ into Eq. (30) and integrating this equation from $\tau = 0$ to $\tau = 2/3$ we then readily obtain, if P at $\tau = 0$ is neglected,

$$P(\tau = 2/3) = \int_0^{2/3} \frac{g}{\kappa} \, d\tau = \frac{g}{\kappa_1} \tag{31}$$

where κ_1 is evaluated at $\tau = 2/3$. While the exact value of this integral depends on the assumptions made, it is evident that Eq. (31) must always be correct within a factor of order unity. Substituting this approximation for the integral term in Eq. (29) we obtain, finally, the desired generalization of the shock momentum equation:

$$P_1 + \rho_1 u_1^2 = P_2 + \rho_2 u_2^2 + g/\kappa_1 . \tag{32}$$

We next consider the energy conservation relation for the shock region. The rate at which energy is transported by mechanical means into the shock region at r_2 is given by $\rho_2 |u_2| (H_2 + \frac{1}{2}u_2^2)$, and the rate of mechanical energy transport out of the shock region at r_1 is $\rho_1 |u_1| (H_1 + \frac{1}{2}u_1^2)$. In these expressions $H = E + P/\rho$ is the specific enthalpy of the material and it includes both the internal energy transported by the flow and the work done by pressure forces in the moving fluid. These expressions for the energy transport rates are the same as those occurring in the classical theory of adiabatic shocks, and equating them would yield the energy equation for an adiabatic shock. In the present situation we must include also the radiative energy flux into and out of the shock region; if we denote by F_1 and F_2 the outward radiative energy fluxes per unit area at r_1 and r_2, the energy conservation relation for the shock region then becomes

$$\rho_1 |u_1| (H_1 + \tfrac{1}{2}u_1^2) + F_2 = \rho_2 |u_2| (H_2 + \tfrac{1}{2}u_2^2) + F_1 . \tag{33}$$

(This equation can also be derived by integrating the energy Eq. (26) between r_1 and r_2, neglecting time derivatives and assuming a steady flow as before.)

The term F_1 in Eq. (33) represents the radiative energy flux outward from the interior of the core and is known given the interior structure of the core, being related to the temperature gradient in the outer layers of the core through Eq. (27). If convective energy transport is important at the surface of the core, the convective energy flux must be added to the radiative flux F_1. The term F_2 in Eq. (33) represents primarily the flux of radiation emitted outward from the hot region just inside the shock front, but it also contains a small negative contribution due to radiation emitted inward across the shock front from the material outside it; this latter effect is relatively unimportant and will be neglected here. The outward flux F_2 at $r = r_2$ may be significantly less than the outward flux at the shock front ($r = R$) if there is a large optical depth between R and r_2; however, since the choice of r_2 is largely a matter of numerical convenience, we can assume for the moment that r_2 is close enough to R that the intervening optical depth is small. The flux F_2 is then just equal to the outward flux at the shock front, which depends on the temperature structure inside the shock front. In the present simple treatment of the shock region, only the single parameter T_1 is available to specify the temperature distribution inside the shock front; therefore we require some approximation to relate F_2 to T_1.

It will be convenient to define an effective temperature T_e for the shock front by setting $F_2 = \sigma T_e^4$; the problem is then to relate T_e to T_1. If T_1 represents the asymptotic value to which the temperature inside the shock front falls after radiative cooling has become negligible, it is clear that

we must have

$$T_e > T_1 \ , \tag{34}$$

since T_e represents a sort of mean temperature for the (optically thick) radiating region in which $T \geqslant T_1$. On the other hand, T_e cannot be much greater than T_1 , even if the peak temperature just inside the shock front becomes orders of magnitude larger than T_1 , as is the case during the final stages of the collapse. This is because the hot layers inside the shock front emit an outward radiative flux of σT_e^4 (by definition), and they must also emitaa similar amount of energy in the *inward* direction; therefore the radiation intensity inside the shock front must be comparable with that of a blackbody of temperature T_e , so that the minimum temperature T_1 cannot be much smaller than T_e . In fact, it can be demonstrated (Larson 1969a) that in the case of a grey opacity T_1 must lie within the limits

$$0.78\ T_e < T_1 < T_e \ . \tag{35}$$

Thus the error in T_1 will not exceed ~20% if we adopt the simple approximation

$$T_1 = T_e \ , \tag{36}$$

which is consistent with our earlier identification of the surface $r = r_1$ with the photosphere of the stellar core where $T_1 = T_e$. If we accordingly set $F_2 = \sigma T_e^4 = \sigma T_1^4$, we finally obtain the desired form of the energy conservation relation for the shock region:

$$\rho_1 |u_1| (H_1 + \tfrac{1}{2}u_1^2) + \sigma T_1^4 = \rho_2 |u_2| (H_2 + \tfrac{1}{2}u_2^2) + F_1 \tag{37}$$

where F_1 is evaluated as indicated following Eq. (33).

In order to relieve the numerical method of the necessity of handling the steep temperature rise which can occur in a thin region immediately outside the shock front if the infalling material is optically thick, it is sometimes convenient to choose the point r_2 to be at a finite distance (but still less than one grid zone) outside the shock front. If there is a large optical depth τ between R and r_2 , the radiative flux F_2 at r_2 may be substantially smaller than σT_1^4 . While the relevant radiative transfer problem has not been solved, a limit can be set to the reduction factor by neglecting the re-emission of radiation between R and r_2 ; the flux is then reduced by a factor $e^{-\tau}$ between R and r_2 , so that we have $F_2 = e^{-\tau}\sigma T_1^4$. It turns out, however, that the insertion of a factor $e^{-\tau}$ makes no difference to the final results, since the layers just outside the shock front become optically thin anyway at an early stage in the evolution of the stellar core.

Eqs. (28), (32), and (37) now provide the three 'shock jump conditions' required to relate the values of the flow variables u_1 , ρ_1 and T_1 inside the shock front to their values u_2 , ρ_2 , and T_2 outside the shock front.

11 TREATMENT OF THE TEMPERATURE DISTRIBUTION IN THE INFALLING CLOUD

After the formation of the stellar core, the radiation emitted from the shock front at the surface of the core begins to heat up the outer parts of the protostellar cloud. The assumption that the outer optically thin region remains nearly isothermal is then no longer valid, and a more detailed consideration of the radiative transfer problem and the temperature distribution in the infalling protostellar envelope is required. Since the infalling cloud extends over several orders of magnitude in radius, it is essential to take the spherical geometry into account. At present, detailed solutions of the radiative transfer problem in an extended spherical 'atmosphere' are available only for the special case of a grey atmosphere with a density distribution of the form $\rho \propto r^{-n}$ (e.g., Hummer and Rybicki 1971). For a protostar the assumption of a grey opacity is not likely to be closely satisfied; however, since the non-grey case is much more complicated to treat and since the dynamical results are in any case not very sensitive to the details of the temperature distribution, the assumption of a grey opacity may provide a reasonable first approximation for purposes of calculating the dynamics. The assumption of a power law density distribution in a collapsing protostellar envelope is in fact a good one, since during the later stages of the collapse the density distribution is closely approximated by $\rho \propto r^{-3/2}$ throughout most of the infalling cloud (see Section 12(c)).

It has been shown by Hummer and Rybicki (1971) that a good approximation to the exact solution for the source function J in an extended spherical atmosphere in which $\kappa\rho \propto r^{-n}$ can be obtained by adding together the simple analytic expressions for J which hold in the limits of large and small optical depths. If we assume pure thermal emission and absorption by the dust grains and neglect scattering (a good approximation at infrared wavelengths), then J is proportion to T^4 and we can obtain a close approximation to the temperature distribution throughout the cloud by adding together the expressions for T^4 holding at large and small optical depths. In the case of a density distribution of the form $\rho \propto r^{-3/2}$ the maximum error in this approximation is only about 13% in T^4 , or 3% in T (Hummer and Rybicki 1971).

Adopting this method of approximating the temperature distribution, it is possible to derive a simple formula which can replace the radiative diffusion Eq. (27) in the dynamical calculations and which will yield approximately correct temperatures at all optical depths. We consider first the expressions

for T^4 holding at large and small optical depths. In the limit of large optical depths radiative transfer is described by the diffusion Eq. (27); rewriting this to yield an expression for T^4, we obtain

$$T^4 = -\frac{3\kappa\rho TL}{64\pi\sigma r^2}\left(\frac{dT}{dr}\right)^{-1} . \qquad (38)$$

In the limit of small optical depths, i.e. at large distances from the center of the cloud, the radiation field approaches that of a point source of luminosity L at distance r. For a grey opacity the temperature is then independent of the opacity and is given by

$$T^4 = \frac{L}{16\pi\sigma r^2} . \qquad (39)$$

To obtain an approximation to the temperature distribution which is valid at all optical depths we now add together expressions (38) and (39) for T^4. The resulting equation can be rewritten in a form analogous to the diffusion equation relating L to the temperature distribution:

$$L = -\frac{64\pi\sigma r^2 T^3}{3\kappa\rho}\frac{dT}{dr}\left[1+\frac{4}{3}\frac{dT}{\kappa\rho T\,dr}\right]^{-1} . \qquad (40)$$

A slightly modified form of Eq. (40) was used by Larson (1972b) in computing dynamical models for collapsing protostars.

For purposes of computing the emitted spectrum of a protostar the grey approximation is not adequate, since the spectrum is quite sensitive to the wavelength dependence of the opacity. An approximate solution for the temperature distribution in the non-grey case was obtained by Larson (1969b) using a method similar to that employed here; this will be described in more detail in Section 15 in connection with the observed properties of protostars. Meanwhile we note that comparison of grey and non-grey solutions for the temperature distribution shows differences which at worst do not exceed a factor of 2; this may be taken as an indication of the maximum error which can arise from using the approximation described in this Section. As was mentioned earlier, the effect of this error on the dynamics is probably not severe, especially when compared with the many other uncertainties affecting the calculations.

A different and more elaborate treatment of radiative transfer in the outer layers of a protostar has been employed by Narita *et al.* (1970). This method, which involves computing the radiation intensity $I(r, \theta)$ as a function of both the position r and the direction θ, is in principle more accurate than the simple approximation employed here; however, because of the computational complexities, it has not yet been applied in calculating the evolution of protostars whose envelopes are as extended as those considered here.

12 LATER EVOLUTION OF A PROTOSTAR OF ONE SOLAR MASS

A. Expansion of the stellar core

Calculations of the stages of evolution following the formation of the stellar core have been carried out by Larson (1969a, 1972b); we shall describe here the principal results. When the stellar core first forms, the density of the material in the core and just outside it is so high that radiative energy transport is negligible and the flow into the core is adiabatic. In particular, the shock front at the surface of the core is initially adiabatic, the radiative energy flux across it being negligible compared with the mechanical energy flux. As material falls into the stellar core, the density and pressure just outside the shock front drop rapidly, and because of the shock momentum Eq. (32) the density and pressure in the outer layers of the core also decrease rapidly, causing the core to expand. Soon a point is reached where the layers just outside the shock front are no longer completely opaque and radiation begins to carry a significant amount of energy away from the shock front. When radiative energy losses from the surface of the core become important, the core stops expanding and begins to contract.

The stellar core reaches its maximum radius at a time about 1 year after the formation of the core; at this time the mass and radius of the core have both increased by about an order of magnitude to about $0.01\ M_\odot$ and $15\ R_\odot$ respectively. These numbers are somewhat uncertain since they depend on the opacity of the layers immediately outside the shock front; this opacity is not very well known because in the relevant temperature range ($\approx$2000–2500°K) the dust grains have evaporated and molecules make a large but uncertain contribution to the opacity (Tsuji 1971). Nevertheless, experimentation with large changes in the assumed opacity (Larson 1972b) has shown that in all cases, significant radiative energy losses from the shock front begin to occur within a few years after the formation of the stellar core, i.e. at a time when the core mass still is only about $0.01\ M_\odot$. After this point essentially all of the energy emitted from the shock front is effectively radiated away, although it does not immediately leave the protostellar cloud but is first absorbed by the dust grains in the cooler outer regions of the cloud, from which it is re-emitted thermally at infrared wavelengths. This infrared radiation is then efficiently transported out of the protostellar cloud, so that the infrared luminosity of the protostar is the same as the luminosity emitted from the

shock front.

The evolution of the stellar core in an HR diagram is illustrated for a protostar of one solar mass in Figure 7. The initial adiabatic phase of evolution is represented by the dashed section of the curve; the luminosity indicated by the dashed curve is not observed, however, since this energy does not escape from the protostar. The point where 90% of the energy emitted from the surface of the stellar core begins to escape from the protostar as infrared radiation is indicated by the beginning of the solid curve.

At the end of the short adiabatic phase of evolution, most of the mass which originally formed the first core has fallen into the second (stellar) core. The first shock front is still in existence but is beginning to die out as material falls away from it. The time elapsed is still too short for any significant dynamical changes to have taken place outside the first shock front, where most of the protostellar mass still lies. However, the infalling cloud is rapidly heated to temperatures well above 10°K, as given by Eq. (40), as soon as radiation begins to escape from the immediate vicinity of the shock bounding the stellar core.

B. Cooling and contraction of the core

When radiative energy losses form the shock front first become important, the specific entropy of the material entering the stellar core begins to drop, causing the core radius to decrease. (For a discussion of the relation between entropy and core radius, see Appendix A.) Also, the entropy gradient in the outer part of the core becomes negative, and therefore this region becomes unstable to convection and a convection zone appears. Meanwhile the density and pressure at the surface of the core continue to drop, with the result that the opacity of the surface layers decreases and radiative energy transport starts to become important near the surface of the core. The core then begins to lose a significant amount of energy, which is carried by convection from the interior of the core and then radiated away from the surface. The outward energy flow from the interior soon becomes the dominant energy flux at the surface of the core, which thus assumes the character of a stellar atmosphere. The structure of the core at this time is similar to that of a conventional 'Hayashi' model for a pre-main sequence star with an outer convection zone (Hayashi *et al.* 1962), and the core proceeds to evolve along a 'Hayashi track' in the HR diagram, as represented in Figure 7 by the section of the curve between about 10 and 100 years. However, the mass of the stellar core is still very small at this time ($\sim 0.01\ M_\odot$), so that its Hayashi track occurs at a lower effective temperature (~ 2700°K) than for a conventional pre-main sequence star of one solar mass.

As the core contracts and grows slowly in mass, the infall velocity and hence the kinetic energy of the infalling material increase with time, while

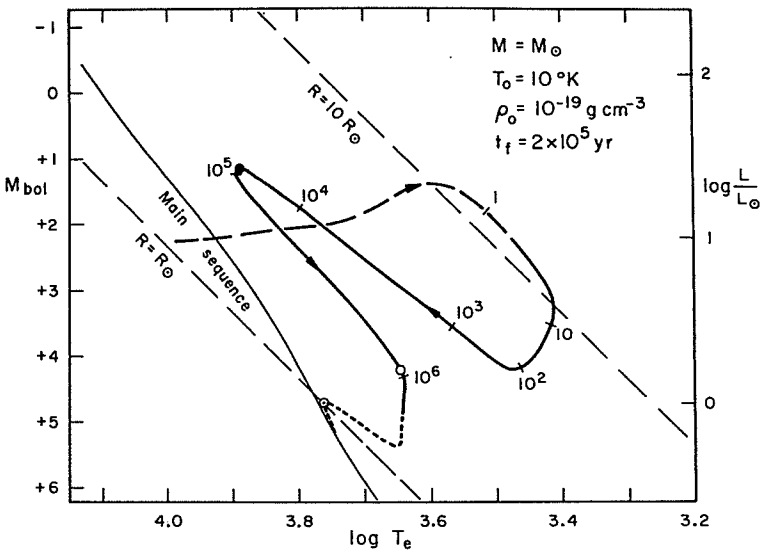

FIGURE 7 The evolution of the stellar core in the HR diagram for a protostar of mass $1\ M_\odot$. The numbers marked along the track give the time in years since the formation of the stellar core. The solid dot represents the point where half of the total mass has been accreted on the core, and the open circle represents the point where the optical depth of the infalling envelope drops below unity and the stellar core becomes visible as a newborn pre-main sequence star. (From Larson 1972b.)

the energy outflow from the interior of the core decreases. After the core has contracted by about a factor of 2 in radius, the kinetic energy inflow becomes the dominant energy input to the shock region. The effective temperature of the core then begins to rise significantly above that corresponding to the 'Hayashi track' and the specific entropy of the material entering the core stops decreasing and begins to increase, halting the contraction of the core and causing the convection zone to disappear. At this time, which occurs about 100 years after the formation of the stellar core, the core radius is about $5\ R_\odot$ and its mass is still close to $0.01\ M_\odot$. By this time all traces of the first core and of the shock front bounding it have disappeared, the material having fallen into the second (stellar) core. At this stage and afterward practically all of the protostellar mass is either in the stellar core or in the outer part of the infalling cloud where the material has not yet had time to fall inward very far; very little mass remains in the intervening region, which extends over some orders of magnitude in radius.

C. Density distribution in the infalling cloud

Once all traces of the first core have disappeared, the density distribution in the inner 'evacuated' part of the infalling cloud closely approaches the simple form $\rho \propto r^{-3/2}$. This may be understood as follows. Since the amount of mass in the inner part of the cloud is negligible, the mass flux must be constant (independent of r) throughout this region; thus

$$4\pi r^2 \rho u = \text{const.} \tag{41}$$

Since the material is essentially in free fall, we also have

$$\tfrac{1}{2}u^2 = \frac{GM}{r} \tag{42}$$

where M is the mass of the stellar core. Substituting $u \propto r^{-1/2}$ into Eq. (41), we then find

$$\rho = \rho_0 r^{-3/2} . \tag{43}$$

In the outermost part of the cloud the density distribution still has approximately the form $\rho \propto r^{-2}$ resulting from the initial isothermal phase of the collapse; However, as the collapse proceeds and more material falls into the stellar core, the region in which Eq. (43) applies expands outward, eventually occupying almost the whole infalling cloud. The evolution of the density distribution in the infalling cloud is illustrated in Figure 8 where the curves are labeled with the logarithm of the time in years since the formation of the stellar core. The disappearance of the first core after ~ 10 years is evident, as is the steady decrease in ρ_0 as the cloud becomes depleted of material.

The applicability of Eq. (43) is not necessarily restricted to the spherical collapse problem considered here, but may also extend to more general circumstances. This has been shown by Hunt (1971), who has solved numerically the accretion problem for an object moving supersonically through a surrounding medium of uniform density. For the equation of state considered, i.e. $P \propto \rho^{5/3}$, it was found that near the accreting object the increase in pressure caused by the converging flow is sufficient to make the inflow radially symmetric; the density distribution is then once again described by Eq. (43) near the accreting object.

D. Later evolution of the stellar core

The evolution of the stellar core is governed by the rate at which material falls into it and by the physical properties of the incoming material after passing through the shock front at its surface. The properties of the shock front

depend in turn on the density and velocity of the infalling material; its temperature is relatively unimportant, since the thermal pressure and energy of the infalling gas soon become negligible compared with the dynamical pressure and the kinetic energy. Since the infall velocity depends on the mass and radius of the core through Eq. (42), there is only one independent variable governing the evolution of the core, which can be taken either as the density of the infalling material or as the mass inflow rate. This is fortunate since it means that the later evolution of the stellar core can be treated without reference to the detailed properties of the infalling protostellar envelope, except insofar as they affect the accretion rate.

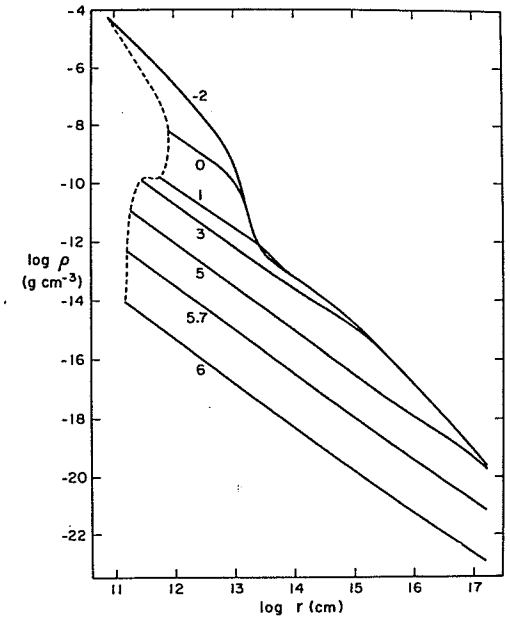

FIGURE 8 The density distribution throughout the infalling enevelope at several times during the evolution of a protostar of $1\ M_\odot$. The dotted curve represents the locus followed by the surface of the stellar core, and the numbers marked on the curves give the logarithm of the time in years since the formation of the stellar core.

During the later evolution of the stellar core, most of the terms in the energy conservation relation (37) for the shock region become small compared with the two dominant terms, i.e. those representing the kinetic energy inflow and the radiative energy outflow from the shock; Eq. (37) then reduces to

$$\sigma T_1^4 \cong \sigma T_e^4 \cong \tfrac{1}{2}\rho_2 |u_2|^3 . \tag{44}$$

Thus the surface temperature T_e of the stellar core is determined by the condition that essentially all of the kinetic energy of the infalling material is converted into radiation in the shock front. As the core mass increases, the infall velocity u_2 increases in accordance with Eq. (42), and the increase in $|u_2|^3$ initially overbalances the decrease in the infall density ρ_2 and causes the effective temperature T_e and the luminosity $L = 4\pi R^2 \sigma T_e^4$ of the core to increase with time, as determined by Eq. (44). The increase in T_1 inside the shock front causes the specific entropy of the material entering the core to increase with time, which tends to increase the radius of the core (see Appendix A); on the other hand, the increase in the core mass has the opposite effect of tending to decrease the radius, and the net effect is that the radius of the core remains nearly constant as it grows in mass. This phase of evolution is represented in Figure 7 by the section of the evolutionary track between about 10^2 and 10^5 years. Approximately half of the total protostellar mass is accreted on the core during this phase of evolution.

The solid dot in Figure 7 indicates the point at which half of the total mass has been accreted on the stellar core; at this time, which occurs about 7×10^4 years after the formation of the core, the radius of the core is about $3\ R_\odot$, its effective temperature is about 8000°K, and its luminosity is about $25\ L_\odot$. The structure of the core at this time is determined mainly by the entropy distribution in the outer layers which have been acquired by accretion during the later stages of the accretion process, i.e. between 10^2 and 10^5 years after the formation of the core. Since radiative energy transport is negligible in the interior of the core, each fluid element retains the specific entropy imparted to it on passage through the shock front, and the structure of the core is therefore determined primarily by the properties of the shock front during the later stages of the accretion process. The material acquired during the earliest stages of formation of the core has a much smaller specific entropy, reflecting the low entropy of the matter from which the core formed; however, after 10^5 years the initial core material constitutes only a small fraction of the mass and volume of the core, and its properties hardly make any difference to the structure of the rest of the core. Thus the details of the formation and early evolution of the core, including the various uncertainties which arise during this stage, have little effect on the later evolution of the stellar core; the later evolution of the core and the properties of the resulting pre-main sequence star are determined mainly by the infall rate during the later stages of the accretion process.

After slightly more than half of the total protostellar mass has been accreted on the core, the rate of increase of the infall velocity u_2 becomes insufficient to keep the kinetic energy inflow rate in Eq. (44) increasing; the continuing decrease in the density ρ_2 then begins to dominate, and the kinetic energy inflow rate begins to decrease. The effective temperature and luminosity of the core then also begin to decrease in accordance with Eq. (44). In addition,

the specific entropy of the material entering the stellar core begins to decrease, with the result that a convection zone appears at the surface of the core and begins to grow inward. The decrease in the surface temperature of the core causes a decrease in the opacity and allows radiative energy transport to become important near the surface of the core; together with the convective energy transport taking place deeper in the interior of the core, this causes the core to lose energy and to contract somewhat as it cools. The kinetic energy inflow to the shock front continues to decrease as the infalling envelope becomes depleted of material, and when nearly all of the protostellar mass has fallen into the core, the kinetic energy inflow becomes unimportant compared with the convective and radiative energy outflow from the interior of the core. The stellar core then becomes a normal pre-main sequence star of one solar mass, and its surface layer becomes a stellar atmosphere in which infall no longer plays a dominant role. The position of the stellar core in the HR diagram at this time is indicated by the open circle in Figure 7, which represents the point at which the visual optical depth of the infalling cloud drops to unity and the newly formed pre-main sequence star first becomes visible.

When the stellar core first becomes visible as a pre-main sequence star, it has a convection zone extending over roughly the outer half of its mass and radius, and it lies quite close to the classical Hayashi track for the convective phase of pre-main sequence evolution. However, it appears near the lower end of the Hayashi track with a radius of only about $2\ R_\odot$, an effective temperature of about 4400°K, and a luminosity of about $1.5\ L_\odot$. These properties place the newly formed star in the middle of the region of the HR diagram occupied by the T Tauri stars (Herbig 1962), which is consistent with the generally accepted interpretation of the T Tauri stars as newly formed stars. The time elapsed between the formation of the stellar core and the appearance of the final T Tauri star is about 9×10^5 years, or about 4 times the free fall time of the initial cloud; the time elapsed since the beginning of the collapse is about 1.2×10^6 years, or about 6 free fall times.

The position of the newly formed T Tauri star in the HR diagram depends on the initial and boundary conditions assumed for the collapsing protostar. For example, if for some reason Eq. (2) is inapplicable and the radius of the protostellar cloud is a factor of 10 smaller than has been assumed, the radius and luminosity of the resulting star are increased to about $6\ R_\odot$ and $9\ L_\odot$ respectively, and the total formation time is reduced to about 3.5×10^4 years (Larson 1969a). This is perhaps an extreme case, but variations of at least a factor of 2 in the radius and a factor of 4 in the luminosity of the resulting star can plausible result from variations or uncertainties in the initial and boundary conditions (Larson 1972b). This may account for some of the observed scatter of the T Tauri stars and other pre-main sequence stars in the HR diagram.

E. The results of Hayashi and collaborators

Even more extreme results have been found in the calculations of Hayashi and his collaborators (see Narita *et al.* 1970 and references), who started their collapse calculations with initial configurations of much higher density than we have considered up to now. For example, for a $1\ M_\odot$ protostar model, Narita *et al.* (1970) begin with a polytropic sphere of index 4 whose radius is only $5 \times 10^3\ R_\odot$, its central density is then 7×10^{-9} g cm^{-3} and its mean density is 1×10^{-11} g cm^{-3}, about 8 orders of magnitude higher than the initial density of $\sim 10^{-19}$ g cm^{-3} indicated by the Jeans criterion (Section 4). This choice of starting configuration for the collapse calculations was made because Narita *et al.* assumed that when a protostar collapses to sufficiently high densities it becomes completely opaque throughout, and that its structure at the beginning of the opaque phase can be adequately approximated by a polytropic sphere. However, the collapse calculations which we have described in Sections 5 and 9 show that the early stages of the collapse are much more nonhomologous than was anticipated by Narita *et al.*, so that only a very small region at the center becomes opaque and most of the mass remains behind in an extended optically thin region of much lower density; the resulting structure is very different from a polytropic sphere. Thus the assumptions of Narita *et al.* do not appear to be justified on the basis of present calculations of the early stages of collapse of a protostar. However, since we cannot conclusively rule out the possibility that, for reasons not yet understood, a protostar may be compressed to a density very much higher than that give n by the Jeans criterion before it begins to collapse freely, we shall briefly describe the results of Narita *et al.* as an example of what might happen under such extreme conditions.

Even though the models of Narita *et al.* (1970) are opaque and they collapse adiabatically rather than isothermally, the results show qualitatively the same type of nonhomologous behavior as was described in Section 5. After about 1/2 year has elapsed, the central pressure becomes high enough to stop the collapse at the center and a small 'stellar core' in hydrostatic equilibrium is formed; as before, the core is bounded by a shock front in which the infalling material is brought almost to rest. The core initially contains a few percent of the total mass and has a radius of a few $R_\odot$, but its mass and radius grow rapidly as more material falls into it. After about 2 years, the core contains about 95 percent of the total mass and has a radius of approximately $100\ R_\odot$. At this point, the optical depth of the layers outside the shock front becomes small enough to allow a large amount of radiation to escape from the surface layers of the core, and the protostar brightens rapidly within about one day to a luminosity of the order of $10^3\ L_\odot$. Within about 10 years most of the remaining material falls into the core and the core begins to settle into a convective configuration located near the top of the 'Hayashi track' in the HR diagram.

At present, no observed objects have been shown to be explained by the calculations of Narita *et al.* (1970); rather, as will be mentioned briefly in Sections 15 and 16, most of the observations believed to relate to very young or newly formed objects seem to be in better agreement with the results of the calculations described earlier. This suggests that the initial conditions assumed by Narita *et al.* are too extreme and that the actual initial conditions for protostars are, as expected from the discussion in Sections 2–4, closer to what would be estimated from the Jeans criterion.

13 EVOLUTION OF MORE MASSIVE PROTOSTARS

According to the results of Larson (1972b), the evolution of protostars with masses between $0.25\ M_\odot$ and $1.5\ M_\odot$ is qualitatively very similar to that already described in Section 12 for a protostar of $1\ M_\odot$. The main difference in the results for different masses is that the effective temperature and luminosity of the resulting T Tauri star increase gradually with increasing mass, varying from about 3700°K and $0.5\ L_\odot$ respectively for a star of mass $0.25\ M_\odot$ to about 4700°K and $3\ L_\odot$ respectively for a star of mass $1.5\ M_\odot$. In all cases the radius of the resulting newborn star is close to $2\ R_\odot$, so that the predicted positions of newborn stars fall along a line in the HR diagram corresponding to a nearly constant radius of about $2\ R_\odot$, again in general agreement with the observed properties of the T Tauri stars.

For a protostar of mass $1.5\ M_\odot$, the resulting star first appears almost at the bottom of its Hayashi track, and the convective 'Hayashi phase' of pre-main sequence evolution is almost non-existent; the star begins to evolve toward the main sequence along a 'radiative' track almost immediately after it is formed. For a protostar of mass $2.0\ M_\odot$, as illustrated in Figure 9, there is no real Hayashi phase at all, and radiative energy transport becomes important in the interior of the core even before all of the protostellar mass has been accreted on it. About 1.2×10^6 years after the formation of the stellar core, at which time the infalling envelope has a mass of about $0.01\ M_\odot$ and an optical depth of about 3, radiation begins to transport energy at a significant rate from the central part of the core to its outer layers, causing the outer layers to heat up and expand. As the outer part of the core comes into radiative equilibrium with the energy flux from the interior, the core brightens rapidly from about $15\ L_\odot$ to $25\ L_\odot$ within only a few days. Once the core has settled into a radiative equilibrium configuration, it begins to contract and evolve toward the main sequence along a 'radiative track'. The optical depth of the infalling cloud finally drops below unity during this phase of evolution; the effective temperature of the core is then about 6800°K and its luminosity about $30\ L_\odot$. At this point the time elapsed since the formation of the core is about 1.4×10^6 years.

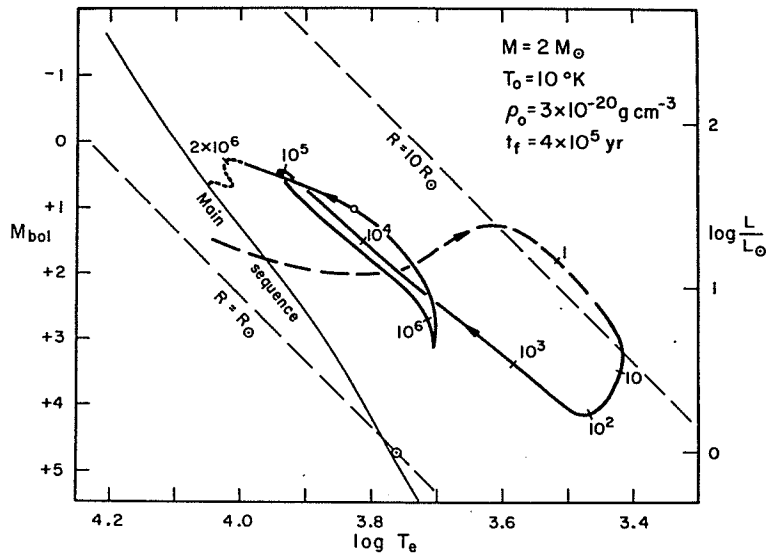

FIGURE 9 The evolution of the stellar core in the HR diagram for a protostar of mass $2\,M_\odot$. (From Larson 1972b.)

Protostars with masses greater than $2\,M_\odot$ all experience a phase of evolution corresponding to that just described, during which radiative energy transport from the hot interior of the core causes the outer layers to heat up and expand as they approach radiative equilibrium. For the more massive protostars this occurs at an earlier stage in the accretion process, i.e. when a substantial fraction of the protostellar mass still remains in the infalling cloud and most of the luminosity of the protostar is still produced by the kinetic energy inflow to the shock front. Since the expansion of the core causes a reduction in the initial velocity (Eq. (42)), it is accompanied by a drop in the kinetic energy inflow rate and hence in the luminosity of the protostar. For a protostar of $5.0\,M_\odot$, this phase of rapid core expansion and decreasing luminosity occurs between about 7×10^4 and 1.1×10^5 years after the formation of the core, at which time the core mass is about $2.5\,M_\odot$. As the outer layers of the core come into radiative equilibrium, the core brightens rapidly and then begins to contract and evolve toward the main sequence along a radiative track. However, its evolution still differs from classical calculations of pre-main sequence evolution in that it is still growing in mass by accretion, and much of its luminosity is still supplied by the infall of matter into the shock front.

For protostellar masses much greater than about $3\,M_\odot$, the pre-main sequence contraction time for the stellar core becomes shorter than the time required for all of the protostellar envelope to be accreted, so that the stellar

core evolves all the way onto the main sequence while still surrounded by an optically thick cloud of infalling material. For example, in the $5.0\,M_\odot$ calculation illustrated in Figure 10, the stellar core evolves onto the main sequence about 5×10^5 years after it is formed, when its mass is about $4.6\,M_\odot$; at this time the infalling cloud still has a mass of about $0.4\,M_\odot$ and a visual optical depth of about 30. If the continuing infall of matter is not impeded by radiation pressure or other effects, it will continue for at least another 5×10^5 years, during which time the central stellar object evolves up the main sequence as its mass increases to its final value of $5.0\,M_\odot$. Thus a star with a mass of the order of $5\,M_\odot$ or more should already be a main sequence star by the time it first becomes visible through its remnant protostellar envelope. Stars more massive than $5\,M_\odot$ should never be visible as pre-main sequence stars at all, since they remain heavily obscured by their protostellar envelopes until they have already reached the main sequence. This prediction is consistent with the observed paucity or absence of very luminous pre-main sequence stars with masses exceeding about $5\,M_\odot$.

In reality, the final phases of the accretion process for a protostar of mass greater than about $3\,M_\odot$ are likely to be influenced by the effects of radiation pressure and possibly also by mass ejection from the central star. Both of these effects are difficult to treat quantitatively, and therefore they have not yet been incorporated in any of the model calculations. However, it is easily demonstrated that for masses greater than about $3\,M_\odot$ radiation pressure must eventually become dominant over gravity when the infalling cloud becomes optically thin. In an optically thin region, the ratio of radiation pressure to gravity is independent of the distance from the central star and is given by

$$\left| \frac{\text{radiation pressure}}{\text{gravity}} \right| = 7 \times 10^{-5} \kappa \, \frac{L/L_\odot}{M/M_\odot} . \qquad (45)$$

Assuming that the visual opacity of the protostellar material is 250 $\text{cm}^2\ \text{g}^{-1}$, we find from Eq. (45) that radiation pressure is dominant over gravity if

$$\frac{L/L_\odot}{M/M_\odot} \gtrsim 50 , \qquad (46)$$

which occurs for masses greater than about $3\,M_\odot$. For such stars the accretion process must eventually be cut off after the cloud becomes optically thin. Eq. (46) does not hold while the cloud is still optically thick, because the luminosity is then emitted at infrared wavelengths for which the opacity κ is much smaller.

The effects of radiation pressure may become important even before the circumstellar cloud has become optically thin if the radiation pressure acting on the inner part of the cloud becomes comparable with the dynamical pressure of the infalling material. The innermost part of the cloud will contain no dust because the temperature there is high enough to evaporate the dust grains; thus the radiation from the stellar core will first be significantly absorbed or scattered at the inner edge of an outer dust-containing shell in which the temperature is low enough for dust grains to exist. To determine when radiation pressure becomes important for the dynamics of the collapse, we must compare the radiation pressure $L/4\pi r^2 c$ at the inner edge of the opaque dust shell with the dynamical pressure ρu^2 of the infalling material at this point†. For example, if we assume that the dust grains evaporate at 2000°K and examine the results obtained for a protostar of $5\ M_\odot$, we find that radiation pressure becomes competitive with the dynamical pressure when the infalling cloud has a mass of about $0.05\ M_\odot$ and a visual optical depth of about 6. What happens after this points remains to be determined by more detailed computations, but it is possible that the dust shell will be disrupted at least temporarily by a Rayleigh-Taylor-like instability. If this occurs, visual radiation will begin to escape from the inner regions of the protostar and, if condition (46) is satisfied, it can blow away the rest of the cloud. The dust shell then will not be replenished by inflow from the outer part of the cloud, and it therefore disappears permanently. The dissipation in this way of an opaque dust shell might lead to a rapid brightening of the protostar similar to what has been observed for the pre-main sequence objects FU Ori and V 1057 Cyg (Larson 1972b), although Grasdalen (1973) has argued against this type of interpretation for these objects (see Section 16).

For protostellar masses greater than $10\ M_\odot$ the dynamical effects of the radiation field of the central stellar core become increasingly important, but also increasingly difficult to treat accurately; for this reason no model calculations are yet available for masses greater than $10\ M_\odot$. These are at least four effects which may become important for massive protostars (Larson and Starrfield 1971): (1) The high luminosity of the stellar core may heat up the outer layers of the infalling cloud to the extent that pressure gradients become large enough to retard or prevent the infall of the outermost layers of the cloud. (2) Radiation pressure acting on the inner edge of the dust shell may become sufficient to impede or halt the accretion process at an earlier stage than in the $5\ M_\odot$ example considered above, i.e. when a substantial fraction of the total mass remains in the infalling cloud. (3) For a very

† The expression given here for the radiation pressure assumes pure absorption by the dust grains and neglects the effect of scattering; the effect of scattering would be to increase the radiation pressure (Faulkner 1970).

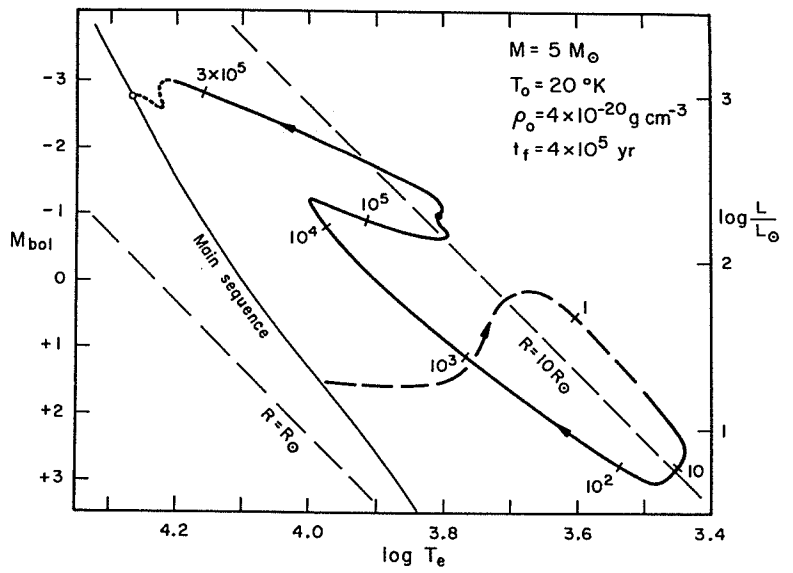

FIGURE 10 The evolution of the stellar core the HR diagram for a protostar of mass $5\ M_\odot$. (From Larson 1972b.)

massive protostar the pressure of infrared radiation on the outer layers of the cloud may become sufficient to blow them off and halt further infall. (4) Eventually, if the above effects do not intervene first, the stellar core of a very massive protostar will become sufficiently luminous at ultraviolet wavelengths to ionize the whole infalling cloud around it. Since the ionization is accompanied by an increase of at least two orders of magnitude in the temperature and pressure, pressure forces then become completely dominant over gravity and quickly blow away the remaining uncondensed gas. Clearly all of these effects will tend to limit the mass which the stellar core can attain before accretion onto it is halted. The implications of this for the upper limit of stellar masses have been discussed by Larson and Starrfield (1971); in the following section we shall briefly review the conclusions which are found concerning the upper limit of stellar masses.

14 THE UPPER LIMIT OF STELLAR MASSES

According to Larson and Starrfield (1971), the dynamical effect of the heating of the outer layers of the protostellar cloud by the luminosity from the stellar core is not important for masses less than $\approx 10\ M_\odot$, but becomes gradually more important for larger masses, for which it may play a significant role in

the dynamics of the collapse. However, because of the uncertainties involved and because of the weak mass dependence of this effect, it does not yield any well defined upper limit to the mass which the stellar core can attain.

The dynamical importance of the radiation pressure acting on the inner edge of the opaque dust shell increases rapidly with increasing mass, and extrapolation to higher masses of the results described in Section 13 indicates that for a total protostellar mass of $40\,M_\odot$, radiation pressure becomes equal to the dynamical pressure when the core has accreted only half of the total mass, i.e. about $20\,M_\odot$. However, infall of matter into the core can continue beyond this point if the infalling material forms dense concentrations or blobs, whose motions will then be less affected by radiation pressure. Thus this effect does not set a firm limit to the mass which the stellar core can attain, but suggests that it will become gradually more and more difficult to build up the mass of the stellar core for core masses exceeding something like $20\,M_\odot$.

The radiation pressure exerted by the infrared radiation from the hot inner part of the protostellar cloud on the outer layers of the cloud is very uncertain owing to the poorly known infrared opacity of the dust grains. Different estimates of the infrared grain opacity indicate that this effect may become important at a core mass anywhere from 25 to $90\,M_\odot$, depending on the opacity. Thus this effect may well be important in limiting the mass which a star can attain, but it is difficult to predict an accurate value for the mass limit.

The effect which appears to be most important in limiting stellar masses is the formation of an H II region in the infalling protostellar cloud when the stellar core has attained a sufficiently high mass and luminosity. The ionization of the cloud will effectively cut off any further infall of material into the stellar core, except perhaps for any small blobs of material which may be dense enough to escape being dispersed by ionization or blown away by radiation pressure. Because of the importance of this effect, both for the formation of massive stars and for the formation of H II regions, we review here how the conditions required for ionization of the protostellar cloud can be estimated.

If $S(r)$ denotes the total flux of ionizing photons across a surface of radius r, we can write the following differential equation for $S(r)$ (Spitzer 1968b, Eq. (54)):

$$\frac{dS(r)}{dr} = -4\pi r^2 x^2 n_H{}^2 \alpha \qquad (47)$$

where x is the degree of ionization, here assumed to be equal to unity throughout the ionized region; n_H is the number density of hydrogen atoms; and $\alpha \cong 2.6 \times 10^{-13}$ cm^{3}s^{-1} is the recombination coefficient for recombinations to the second and higher levels of hydrogen. The size of the ionized

region surrounding a massive stellar core can then be estimated as in the elementary theory of H II regions by integrating Eq. (47) outward from the stellar surface to the point where the ionizing photon flux $S(r)$ drops to zero. Eq. (47) assumes that the H II region is optically thin at wavelengths longward of the Lyman limit; if this is not the case and if Balmer continuum photons contribute appreciably to maintaining the degree of ionization, then the use of Eq. (47) will underestimate the extent of the ionized region and overestimate the core mass at which ionization becomes important.

If the protostellar material consists of 70% hydrogen by mass, we have $n_H = 4.2 \times 10^{23}\rho$. The density distribution $\rho(r)$ throughout much of the protostellar cloud is of the form $\rho = \rho_0 r^{-3/2}$ (Eq. (43)). With these substitutions, Eq. (47) becomes

$$\frac{dS(r)}{dr} = -5.8 \times 10^{35}\ \rho_0^2 r^{-1}\ . \qquad (48)$$

Integrating Eq. (48) from the surface of the stellar core ($r = R_S$) out to the boundary of the H II region ($r = R_{HII}$), defined as the point where $S(r)$ drops to zero, we obtain

$$R_{HII} = R_s \exp\left[\frac{S(R_s)}{5.8 \times 10^{35}\ \rho_0^2}\right] \qquad (49)$$

Because of the exponential dependence of R_{HII} on the flux of ionizing photons emitted by the stellar core, the H II region can be expected to grow rapidly once S reaches a certain critical value depending on ρ_0. To estimate the value of S required to ionize the whole protostellar cloud, we equate R_{HII} to the cloud radius R, which we assume to be given by Eq. (2); we then have $R_{HII}/R_s \sim 10^7$, or $\ln(R_{HII}/R_s) \simeq 16$. From Eq. (49) we then obtain

$$S \simeq 9 \times 10^{36}\ \rho_0^2 \qquad (50)$$

as the number of ionizing photons per second required to ionize the whole cloud.

If for illustration we consider the point in time when half of the total mass has been accreted on the stellar core, we find from the collapse calculations that ρ_0 is given approximately by

$$\rho_0 \simeq 0.05\ MR^{-3/2} \qquad (51)$$

where M is the total protostellar mass. If we substitute in Eq. (51) values of

M and R taken from Table II, we find that ρ_0 is nearly independent of mass for the larger protostellar masses (provided that M and R always satisfy the Jean criterion); for example, ρ_0 varies from 8.9×10^5 g cm$^{-3/2}$ for $M = 380\ M_\odot$ to 1.16×10^6 g cm$^{-3/2}$ for $M = 6.5\ M_\odot$. Adopting a representative value of $\rho_0 = 10^6$ g cm$^{-3/2}$, we find from Eq. (50) that the flux of ionizing photons required to ionize the entire protostellar cloud is approximately

$$S \simeq 9 \times 10^{48}\ \text{s}^{-1} . \qquad (52)$$

From data given by Hjellming (1968) we find that this ionizing photon flux can be produced by a main sequence O star with a mass of about $30\ M_\odot$ and a spectral type of about O 6.5. Thus, under the adopted assumptions, the maximum mass which the stellar core can attain before ionization cuts off further mass accretion is of the order of $30\ M_\odot$.

This limit is increased if the mass of the initial protostellar cloud is more than twice the mass of the final star, since the value of ρ_0 then becomes larger than that estimated from Eq. (51). For example, if the total mass of the collapsing cloud is four times (rather than twice) the mass of the resulting star, the value of ρ_0 is increased by an estimated factor of about 2 over that given by Eq. (51); the value of S required to ionize the cloud then becomes about 3.6×10^{49} s^{-1}, corresponding to a star with a mass of about $60\ M_\odot$ and a spectral type of $\sim$ O 4.5. Note, however, that the mass of the initial collapsing cloud now becomes four times $60\ M_\odot$ or about $240\ M_\odot$, so that a very massive star can form only from the collapse of a cloud whose mass is much larger yet than that of the star to be formed. A further increase in the mass of the cloud can raise the final stellar mass somewhat above $60\ M_\odot$ but probably not by a very large factor; detailed collapse calculations will, however, be required to establish more precise numbers.

It should be noted also that the predicted mass limit is rather sensitive to the assumed initial and boundary conditions for the collapsing protostar; in particular, we see from Eqs. (50) and (51) that the ionizing photon flux S required for complete ionization of the cloud is proportional to R^{-3}. Thus if for any reason the radius of the cloud is smaller than has been assumed, the mass limit is increased. For example, if the initial protostellar cloud has an optical depth smaller than unity, its hydrogen may be mostly in atomic rather than molecular form, as has been assumed up to now; the value of the gas constant $\mathcal{R}$ in Eq. (2) is then increased by a factor of about 1.8, and the cloud radius R is decreased by the same factor, raising the mass limit from $30\ M_\odot$ to about $70\ M_\odot$ (assuming once again that Eq. (51) is applicable). The mass limit will also be influenced by the heating and cooling mechanisms and particularly on the abundances of the heavy elements which provide most of the cooling. For example, depletion of the heavy elements by a factor of 10 increases the initial temperature by approximately a factor of 2, which in

turn reduces the cloud radius by a factor of 2 and raises the limiting mass from $30\ M_\odot$ to about $85\ M_\odot$.

In view of the various uncertainties, it is difficult to predict a precise upper limit for stellar masses, and perhaps no very sharply defined upper limit exists. It appears, however, considering all of the effects which have been discussed, that under normal circumstances it will be difficult to make stars with masses exceeding approximately $60\ M_\odot$, and very difficult, if not impossible, to make stars with masses exceeding ~ 90 or $100\ M_\odot$. This prediction is consistent with the observed upper limit of stellar masses which is of the order of $60\ M_\odot$, except perhaps for a few rare and exceedingly luminous objects like η Carinae, which may be a star with a mass of the order of $100\ M_\odot$.

It is also clear from the above discussion that the formation of massive stars and the formation of H II regions are indissolubly related problems which cannot be treated in isolation. Not only does the formation of an H II region put a halt to the collapse of the cloud, but the collapse process itself determines the initial density distribution in the H II region when it first becomes ionized. Thus, for a spherically collapsing cloud the density distribution will be approximately of the form $\rho \propto r^{-3/2}$ in the inner part of the cloud and $\rho \propto r^{-2}$ in the outer region. The density distribution within the Orion nebula is in fact roughly of this form, and therefore can probably be understood as having been produced by the same collapse process which led to the formation of the Trapezium stars.

15 THE INFRARED EMISSION OF PROTOSTARS

During most of its evolution, the stellar core remains heavily obscured by the dust in the infalling envelope around it, so that the protostar is observable only or primarily as an infrared object. Although the evolution of the stellar core is not very sensitive to the detailed structure of the infalling envelope, the observable properties of the protostar are much more strongly affected by the structure of the envelope. Since calculations are presently available only for the case of a spherically symmetric protostar, we shall discuss in this section the infrared emission from a spherical protostar, but it should be kept in mind that the appearance of the protostar could be rather different if the cloud is not spherical but is asymmetric or flattened. Other uncertainties affecting the results include the gas-to-dust ratio and the poorly known infrared optical properties of the dust grains. Thus it is difficult to predict with quantitative accuracy the infrared appearance of a protostar, and probably only the qualitative results are very significant.

In order to predict the infrared spectrum of a protostar, it is necessary to consider the transfer of infrared radiation through the extended spherical

'atmosphere' of the protostar; here we follow the approximate treatment adopted by Larson (1969b). In common with previous treatments of the radiative transfer problem with spherical symmetry, we assume that the density $\rho(r)$ varies as a negative power of the radius r :

$$\rho = \rho_0 r^{-n} . \tag{53}$$

As we have seen, a law of this form with $n = 3/2$ is a good approximation for the inner part of the infalling protostellar envelope; in fact, the relation $\rho \propto r^{-3/2}$ holds with good accuracy throughout the entire region of interest for the radiative transfer problem. We shall retain a general value of n in most of the equations, substituting $n = 3/2$ at the end in order to obtain numerical results.

A simple first approximation to the temperature distribution throughout the infalling cloud can be obtained by a procedure similar to that used in Section 11, which consisted of adding together the expression for T^4 which hold in the optically thick and optically thin limits. For purposes of calculating the infrared spectrum of a protostar, it is necessary to take into account the non-greyness of the opacity κ_λ , since the assumption of a grey opacity yields an unrealistically broad spectrum (Larson 1969b). In the absence of a good knowledge of the infrared absorption properties of the dust grains, we assume a simple power law dependence of κ_λ on λ :

$$\kappa_\lambda = \kappa_0 \lambda^{-p} . \tag{54}$$

The values $\kappa_0 = 7 \times 10^{-5}$ (cgs) and $p = 3/2$ were found to be consistent with the (scanty) available data for interstellar extinction at near infrared wavelengths (Larson 1969b), but we shall again retain a more general expressions for κ_λ in the formulas to be derived.

In the inner optically thick part of the cloud, radiative transfer is described by the diffusion Eq. (27), where κ denotes the Rosseland mean opacity κ_R . Since the luminosity $L(r)$ is very nearly constant throughout the infalling cloud and since its value is known from the calculations for the evolution of the stellar core, the diffusion Eq. (27), together with Eqs. (53) and (54), can be used to solve analytically for the temperature distribution in the inner optically thick part of the cloud. Using Eq. (54), the Rosseland mean opacity required in this calculation can be evaluated analytically as a function of temperature, and the result is

$$\kappa_R = A \kappa_0 T^p \tag{55}$$

where

$$A = \frac{24\, \zeta(4)}{\Gamma(5-p)\, \zeta(4-p)} \left(\frac{k}{hc}\right)^p \tag{56}$$

and ζ is the Riemann Zeta function. When Eqs. (53) and (55) are substituted into the diffusion equation (27) and the resulting differential equation for $T(r)$ is solved with the conditions $L(r) =$ constant and $T(r) \to 0$ as $r \to \infty$, the result can be written

$$T^4 = B(\kappa_0 \rho_0 L r^{-n-1})^{4/(4-p)} , \tag{57}$$

where

$$B = \left[\left(\frac{4-p}{n+1}\right) \frac{3A}{64\pi\sigma}\right]^{4/(4-p)} . \tag{58}$$

In the case of a non-grey opacity, the temperature of the optically thin outer part of the cloud depends on the spectrum of the radiation emitted from the opaque inner part of the cloud. In the special case of a blackbody spectrum with temperature T_b , the temperature distribution in the optically thin region, as determined by equating the energy absorbed and the energy emitted by the dust grains, is given by

$$T^4 = T_b^{4p/(4+p)} \left(\frac{L}{16\pi\sigma r^2}\right)^{4/(4+p)} . \tag{59}$$

In the more general case of a non-blackbody spectrum, the temperature distribution in the optically thin region will have the same form but with a different numerical constant. We write

$$T^4 = C T_s^{4p/(4+p)} \left(\frac{L}{16\pi\sigma^2}\right)^{4/(4+p)} \tag{60}$$

where C is a constant of order unity and T_s , an approximate 'photospheric temperature' for the protostar, is defined as the temperature at the point where the optical depth is equal to unity at the wavelength of the local blackbody maximum, assuming that the temperature at this point is given by Eq. (57). (This assumption is adopted only for convenience in defining T_s , and does not affect any of the subsequent results.) From Eqs. (53) and (54), the optical depth τ_λ at wavelength λ and radius r is given by

$$\tau_\lambda = \frac{\kappa_0 \rho_0}{n-1} \lambda^{-p} r^{-n+1} . \tag{61}$$

q

Using Eqs. (57) and (61) to solve for the temperature T_s at the point where $\tau_\lambda = 1$ at the wavelength of the local blackbody maximum (defined by $\lambda T_s = hc/4.965k$), we obtain, after some algebra,

$$T_s = [D(\kappa_0\rho_0)^{-1} L^{(n-1)/2}]^{1/(2n+p-2)} \quad (62)$$

where

$$D = \left[(n-1)\left(\frac{hc}{4.965k}\right)^p\right]^{(n+1)/2} B^{(4-p)(n-1)/8}. \quad (63)$$

We can now construct an approximation to the temperature distribution throughout the cloud by adding together the expressions for $T^4(r)$ given by Eqs. (57) and (60) for the optically thick and optically thin regions respectively. Once the temperature is known as a function of radius (or equivalently, as a function of optical depth) throughout the protostellar envelope, the luminosity emitted at any wavelength can be calculated by integrating the contributions from all optical depths, using a procedure quite analogous to that used for a plane parallel stellar atmosphere. Corresponding to the expression

$$F_\lambda = 2\pi \int_0^\infty E_2(\tau_\lambda)\, B_\lambda(\tau_\lambda)\, d\tau_\lambda$$

giving the flux F_λ per unit wavelength interval emitted by a plane parallel atmosphere, we have, in the case of an extended spherical atmosphere in which $\rho \propto r^{-3/2}$,

$$L_\lambda = 16\pi^2 \int_0^\infty r^2(\tau_\lambda)\, G_{3/2}(\tau_\lambda)\, B_\lambda(\tau_\lambda)\, d\tau_\lambda \quad (64)$$

where L_λ is the luminosity emitted per unit wavelength interval, $B_\lambda(\tau_\lambda)$ is the blackbody function, and the function $G_{3/2}(\tau_\lambda)$ is defined and tabulated by Larson (196b). The constant C in Eq. (60) remains an undetermined parameter; however, for any assumed value of C the emitted spectrum of the protostar can be computed by numerical integration using Eq. (64), and C can be varied until the integrated luminosity computed in this way is equal to L, as required. With $n = 3/2$, the values of C determined in this way for $p = 1$, 3/2, and 2 are equal to 1.75, 2.36, and 2.34 respectively. The spectrum computed for the case $n = 3/2$, $p = 3/2$ is illustrated in Figure 11, where it is compared with a blackbody spectrum and with the available data for the Becklin-Neugebauer infrared point source in Orion, which may be an opaque protostar with a mass of about $5\ M_\odot$ (Larson 1972b). Both spectra have been positioned to give the best fit to the data. It is seen that

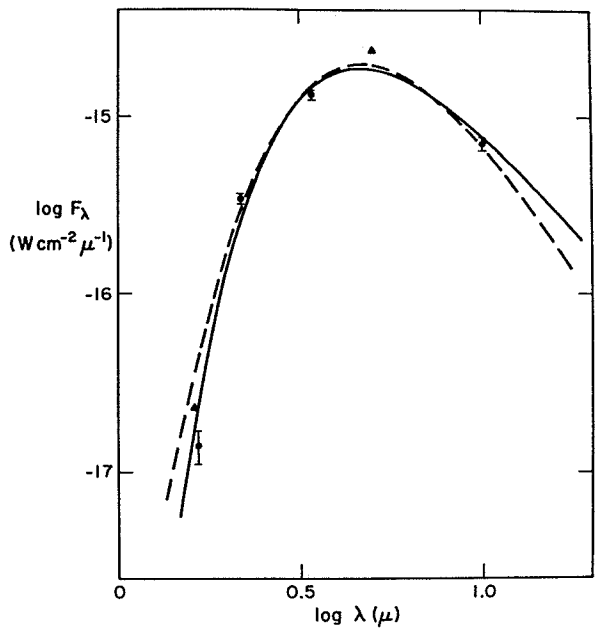

FIGURE 11 The computed spectrum of a protostar for the case $n = 3/2$, $p = 3/2$ (solid curve) and a blackbody spectrum (dashed curve) are compared with observations of the Becklin-Neugebauer infrared point source in Orion. Solid circles with error bars are from Becklin and Neugebauer (1967), corrected for recalibration of the 10μ observation (Becklin, private communication), and the triangles are from Kleinmann and Low (1967).

the computed protostar spectrum is fairly similar to a blackbody spectrum, but it falls off more rapidly than the blackbody spectrum at short wavelengths and less rapidly at long wavelengths. Both spectra give a fairly good fit to the data for the B-N object at most wavelengths, but the observed strong decrease in flux at the shortest wavelength is matched only by the computed protostar spectrum and not by the blackbody spectrum. The spectra calculated for $p = 1$ and $p = 2$ do not fit the observations quite as well as that for $p = 3/2$; the case $p = 1$ yields a broader spectrum than that illustrated, whereas $p = 2$ yields a narrower spectrum.

As a protostar evolves, the peak of the infrared spectrum steadily shifts toward shorter wavelengths as the density of the infalling cloud decreases and the surface of optical depth unity or 'photosphere' moves inward to smaller radii and higher temperatures. Correspondingly, the 'photospheric temperature' T_s increases steadily with time. The wavelength λ_m of peak infrared emission is related inversely to T_s by a relation similar to that for a blackbody, i.e. $\lambda_m T_s$ = constant. From the computed spectra for $n = 3/2$, the values of this constant for $p = 1$, 3/2, and 2 are found to be 0.28, 0.28,

and 0.29 cm °K respectively. Since these values are very close to the blackbody value of 0.290 cm °K, the spectrum peaks at nearly the same wavelength as a blackbody of temperature T_s. The dependence of T_s on ρ_0 and L is given by Eq. (62); for the case $n = 3/2$, $p = 3/2$ this yields

$$T_s = 0.55\ (\kappa_0\rho_0)^{-2/5} L^{1/10} \text{ (cgs units)} \qquad (65)$$

and

$$\lambda_m = 0.51\ (\kappa_0\rho_0)^{2/5} L^{-1/10} . \qquad (66)$$

These equations can be used to predict the variation of T_s or λ_m with time, given the time development of ρ_0 and L which is obtained from the dynamical calculations. For example, if we substitute the representative values $\rho_0 = 10^6$ g cm$^{-3/2}$ and $L = 10^{35}$ erg s^{-1} into Eqs. (65) and (66) and if we assume $\kappa_0 = 7 \times 10^{-5}$, we obtain $T_s = 320$°K and $\lambda_m = 8.8\mu$. Thus typical protostars would be expected to radiate most strongly at infrared wavelengths of the order of 10μ, and to have apparent temperatures of some hundreds of degrees K. It is evident from Eqs. (64) and (65) that these numbers are made somewhat uncertain because of the uncertainty in the dust opacity κ_0.

The time development of the luminosity L and the peak wavelength λ_m for an opaque protostar can be conveniently illustrated by plotting the evolutionary track of the protostar in an infrared HR diagram showing $\log L$ plotted vs $\log \lambda_m$. Such a diagram is shown in Figure 12, taken from Larson (1972b). Evolutionary tracks are illustrated for masses from $0.25\ M_\odot$, and the time scales are indicated by the dashed isochrones. As expected, protostars of low or moderate mass (up to about $2\ M_\odot$) are predicted to be most prominent at wavelengths of the order of 10μ; the evolutionary time scale at this stage is of the order of 10^5 years. These low mass protostars subsequently decline in luminosity as they evolve toward higher apparent temperatures, owing to the decreasing kinetic energy inflow into the shock front. The more massive protostars continue to brighten as they evolve toward higher temperatures, since in these cases much of the luminosity comes from the interior of the core and therefore increases as the core mass increases. In all cases, the total duration of the infrared stage of evolution is predicted to be of the order of 5×10^5 to 10^6 years.

Also shown in Figure 12 are the positions of several objects which are visible only or primarily at infrared wavelengths and which are thought to be protostars or newly formed stars. Since the more massive and luminous protostars spend most of their time at relatively high temperatures and are also most luminous during their later stages of evolution, one would expect luminous protostars to be observed mostly with temperatures of the order of 500 to 1000°K, corresponding to peak wavelengths of about 3 to 6μ; this is in

agreement with the observed properties of many of the infrared objects which are thought to be protostars or newly formed stars.

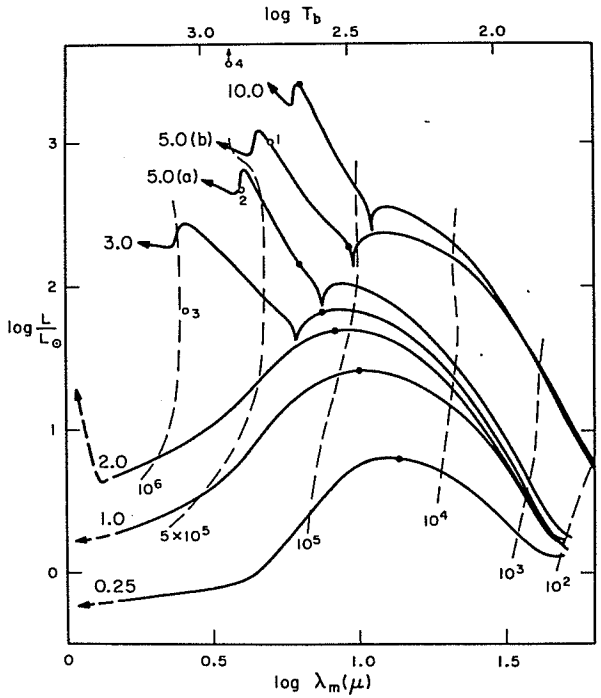

FIGURE 12 Evolutionary tracks of protostars in an infrared HR diagram showing $\log L$ plotted vs $\log \lambda_m$, where λ_m is the wavelength of peak infrared emission. The protostellar masses from $0.25\ M_\odot$ to $10\ M_\odot$ are marked on the curves. The dashed lines are isochrones for the times marked at the bottom. Open circles indicate the positions of (1) the Becklin-Neugebauer object, (2) R Mon, (3) R CrA, and (4) LkHα 101. The solid dot on each curve indicates the point where the stellar core contains half of the total mass. (From Larson 1972b.)

16 PROPERTIES OF T TAURI STARS AND OTHER PRE-MAIN SEQUENCE STARS

The theory of the hydrostatic phase of pre-main sequence evolution has already been thoroughly reviewed by Upton (1968), Cox and Giuli (1968), and Bodenheimer (1972); therefore we shall not attempt any complete discussion of this subject here but merely conclude by pointing out some implications of the collapse calculations described in the preceding sections.

Towards the end of the collapse, the amount of material remaining in the infalling envelope of a protostar diminishes steadily, and after most of this material has either fallen into the core or been dissipated by radiation pressure

or other means, the visual radiation from the central stellar core begins to shine through the surrounding dusty envelope. At first the visual radiation may not escape directly from the cloud but only after scattering from dust grains, so that what is seen from the outside is not the central star itself but rather scattered radiation from the surrounding dusty envelope. In any case, the spectrum of the protostar will begin to show two components, i.e. a visual or 'stellar' component and an infrared component similar to the infrared spectrum from an opaque protostar. A number of such objects are known, the best studied example of which is the T Tauri star R Mon (object 2 in Figure 12), which emits over 90% of its total luminosity at infrared wavelengths. The properties of R Mon can be understood, at least qualitatively, if this object is interpreted as a protostar with a stellar core of mass $\sim 4\ M_\odot$ and effective temperature $\sim 10^4$ °K, surrounded by a remnant protostellar cloud with a mass of perhaps $1\ M_\odot$ which absorbs nearly all of the visual light from the central star and converts it into infrared radiation. The infrared spectrum of R Mon closely resembles that of the Becklin-Neugebauer object in Orion, and is also reasonably well fitted by theoretical spectra computed in the way described in Section 15 (Neugebauer, Becklin and Hyland 1971).

Eventually, after a time of the order of 10^6 years, the circumstellar envelope thins out enough to allow most of the visual radiation from the central star to escape, and the object then radiates predominantly at visual wavelengths with only a small or moderate infrared excess produced by the remnant circumstellar material. Most of the T Tauri stars appear to be identifiable with this stage of pre-main sequence evolution, i.e. the stage when the circumstellar envelope has almost completely disappeared and no longer dominates the observed properties of the star. A good example is the star T Tauri itself, which on photographs is accompanied by only a small wisp of nebulosity, as contrasted with the bright dense cometary nebula around R Mon. Correspondingly, T Tauri has a much less conspicuous infrared excess than R Mon and radiates a smaller fraction of its total energy at infrared wavelengths. Most T Tauri stars have even less infrared emission than T Tauri, although they still show a measureable infrared excess. The more 'normal' T Tauri stars typically have radii of the order of 2 or $3\ R_\odot$ and effective temperatures in the range from about 3500 to 5500°K, in good agreement with the predicted properties of newly formed stars with masses $\lesssim 2\ M_\odot$. The appreciable scatter of the T Tauri stars in the HR diagram, even within a single cluster, may have several causes, among which are differences in the initial conditions for different protostars, differences in the amount of remnant circumstellar obscuration, and a possible age spread of the order 10^7 years (Larson 1972b).

The more massive analogues of the 'classical' T Tauri stars discussed above appear to be found among the relatively luminous Ae and Be stars studied by Herbig (1960) and Strom *et al.* (1972b). According to the collapse calculations described in Section 13, the stellar core in a protostar of mass greater

than about 3 to 5 $M_\odot$ evolves all the way to the main sequence before becoming visible through its obscuring protostellar envelope. Thus newly formed stars with masses larger than this should first appear on or near the main sequence, surrounded initially by a dense and conspicuous cloud of interstellar matter and showing strong infrared emission. These predictions are in good general agreement with the properties of the Herbig Ae and Be stars, all of which are associated with visible nebulosity and most of which lie on or not far from the main sequence. Also, most of these objects show spectroscopic and/or infrared evidence for circumstellar shells. The observations are all consistent with the interpretation of these objects as newly formed stars with masses between $2\ M_\odot$ and $6\ M_\odot$ and ages of the order of 3×10^5 years to 3×10^6 years, which are still surrounded by the remnants of their initial protostellar clouds.

The collapse calculations indicate that the infall of the last remnants of the protostellar cloud into the stellar core may still be going on at a rate of the order of $10^{-7}\ M_\odot$/yr when the star first becomes visible. Therefore one might expect to see some evidence for infall of material in some of the youngest T Tauri stars, provided that the infall has not already been halted by radiation pressure or by a stellar wind. Such evidence has been found by Walker (1972), who has observed redshifted absorption lines in the spectra of certain T Tauri-like stars which he called YY Ori stars. The observed infall velocities of ~ 150 to 400 km s^{-1} are comparable with the expected free fall velocities at the surfaces of pre-main sequence stars with masses $\lesssim 1\ M_\odot$ and radii of a few $R_\odot$. Also, there is evidence that part of the luminosity of the YY Ori stars, particularly in the ultraviolet, is supplied by the infall of matter. Thus the observations appear to be consistent with the interpretation of the YY Ori stars as some of the very youngest T Tauri stars which are still accreting the last remnants of their protostellar envelopes.

The predicted locus of newborn stars in the HR diagram is illustrated in Figure 13, taken from Larson (1972b). The open circles indicate the predicted positions of newly formed stars of various masses at the time when the optical depth of the surrounding cloud becomes equal to unity, and the heavy curve shows the predicted locus of such stars. The dashed curve shows the position of this locus when the radius of the initial cloud is reduced by a factor of 2 for all masses, and the difference between the solid and dashed curves gives an indication of the uncertainty involved. It is seen that the predicted locus of newborn stars falls near the isochrone corresponding to an age of 10^6 years, and that an appreciable scatter in the position of such stars in the HR diagram can result from uncertainties or variations in the initial conditions. These predictions are in fairly good agreement with observations of very young clusters, which show that the pre-main sequence stars generally scatter below an upper envelope which roughly coincides with the dashed curve in Figure 13. The observed scatter probably has a number of causes, including an age spread

of the order of 10^7 years. It is clear that the presence of several sources of scatter precludes a straightforward interpretation of the HR diagrams of young clusters in terms only of the ages and masses of the stars (Strom *et al.* 1971, 1972a; Larson 1972b).

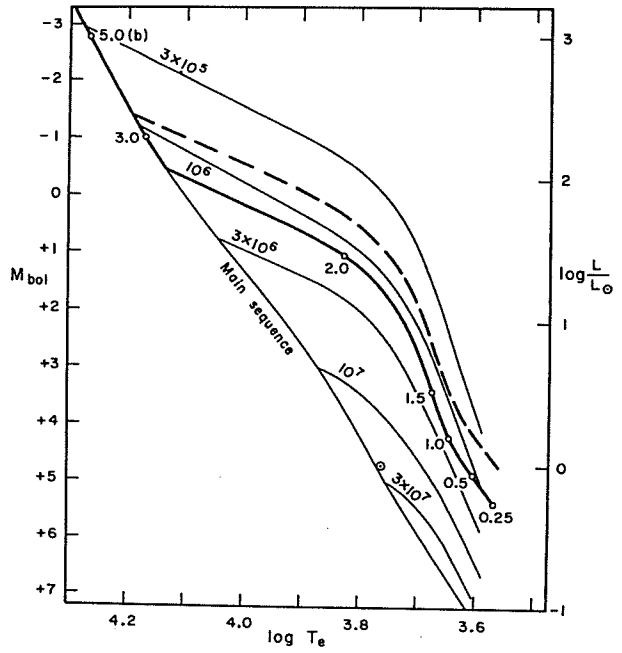

FIGURE 13 The heavy solid curve is the predicted locus along which newborn stars of different masses should first appear in the HR diagram, and the dashed curve shows the position of this locus if the initial radius of the protostellar cloud is arbitrarily reduced by a factor of 2 in all cases. Isochrones from Iben and Talbot (1966) are also shown for reference. (From Larson 1972b.)

Recently, much interest has been generated by the discovery that the object V1057 Cyg, previously identified as a T Tauri star, flared up by about 6 magnitudes within one year in 1969 and then remained nearly constant at the higher luminosity, in a manner reminiscent of FU Ori (see Grasdalen (1973) for a discussion of the properties of V1057 Cyg and its relation to FU Ori and other objects). The evidence strongly suggests that V1057 Cyg is a pre-main sequence star, and according to Grasdalen (1973) it presently has a luminosity of the order of $10^3\ L_\odot$, an effective temperature of about 8000°K, and a mass of about $8\ M_\odot$. It appears to have only a small amount of circumstellar material, in contrast to the Ae and Be stars discussed above. At present the properties of FU Ori and V1057 Cyg are not reproduced quantitatively by any theoretical

model, and it is not even clear whether the great increase in luminosity is to be interpreted as an intrinsic change or as an apparent effect caused by the rapid disappearance of a circumstellar dust shell (although Grasdalen (1973) argues for the former interpretation). The estimated mass and present luminosity of V1057 Cyg are somewhat larger than might be expected for a newly formed star still located well away from the main sequence, if the theoretical results described in Section 13 are correct; according to these results, a star as massive as $8\ M_\odot$ should remain embedded in a dense, opaque protostellar cloud until it has already reached the main sequence. Two possible interpretations of this discrepancy are: (1) the initial protocloud from which V1057 Cyg formed may have been denser than expected from the Jeans criterion, so that it collapsed in a shorter time, or (2) as suggested in Section 13, the protostellar envelope may have been blown away by radiation pressure or a stellar wind before the collapse process was completed. Since both of these possibilities are reasonable ones, considering the uncertainties in the theory, the present properties of V1057 Cyg are not seriously inconsistent with the theoretical picture developed in this article. However, the rapid brightening of FU Ori and V1057 Cyg remains unaccounted for by any detailed quantitative calculations, and it is evident that more theoretical and observational work will be necessary before it can be established what revisions or extensions of the present theoretical picture will be required to fully account for these remarkable objects.

In summary, although the theory of collapsing protostars still contains many uncertainties and much further work remains to be done, it appears that a number of important qualitative or semi-quantitative predictions can be made with reasonable confidence and that these predictions are in reasonable agreement with many of the observations thought to relate to star formation or newly formed stars. Thus it may be hoped that many of the essential qualitative features of the theory outlined in this article will survive when more elaborate and correct treatments of the evolution of protostars are developed.

References

Appenzeller, I. (1972). *Mitt. Astr. Ges.*, **31**, 39.
Bardeen, J.M. (1971). *Astrophys. J.*, **167**, 425.
Becklin, E.E., and G. Neugebauer (1967). *Astrophys. J.*, **147**, 799.
Bodenheimer, P. (1972). *Rep. Prog. Phys.*, **35**, 1.
Bodenheimer, P., and A. Sweigart (1968). *Astrophys. J.*, **152**, 515.
Bok, B.J., C.S. Cordwell, and R.H. Cromwell (1971). In *Dark Nebulae, Globules and Protostars*, B.T. Lynds (Ed.), University of Arizona Press, Tucson, p.33.
Chandrasekhar, S. (1939). *Stellar Structure.* University of Chicago Press.
Cox, J.P., and R.T. Giuli (1968). *Principles of Stellar Structure.* Gordon and Breach, New York.
Disney, M.J., D. McNally, and A.E. Wright (1969). *Mon. Not. Roy. Astr. Soc.*, **146**, 123.
Faulkner, D.J. (1970). *Astrophys. J.*, **162**, 513.

Field, G.B. (1970). In *Evolution Stellaire Avant la Séquence Principale* (16th Liège Symposium), p.29, Université de Liège.
Gaustad, J.E. (1963). *Astrophys. J.*, **138**, 1050.
Goldsmith, D.W., H.J. Habing, and G.B. Field (1969). *Astrophys. J.*, **158**, 173.
Grasdalen, G.L. (1973). *Astrophys. J.*, **182**, 781.
Hattori, T., T. Nakano, and C. Hayashi (1969). *Prog. Theor. Phys.*, **42**, 781.
Hayashi, C., R. Hoshi, and D. Sugimoto (1962). *Prog. Theor. Phys. Suppl.*, No.**22**.
Heiles, C. (1971). *Ann. Rev. Astr. Astrophys.*, **9**, 293.
Herbig, G.H. (1960). *Astrophys. J. Suppl.*, **4**, 337.
Herbig, G.H. (1962). *Adv. Astr. Astrophys.*, **1**, 47.
Hjellming, R.M. (1968). *Astrophys. J.*, **154**, 533.
Hollenbach, D.J., M.W. Werner, and E.E. Salpeter (1971). *Astrophys. J.*, **163**, 165.
Hummer, D.G., and G.B. Rybicki (1971). *Mon. Not. Roy. Astr. Soc.*, **152**, 1.
Hunt, R. (1971). *Mon. Not. Roy. Astr. Soc.*, **154**, 141.
Hunter, J.H. (1969). *Mon. Not. Roy. Astr. Soc.*, **142**, 473.
Iben, I., and R.J. Talbot (1966). *Astrophys. J.*, **144**, 968.
Kellman, S.A., and J.E. Gaustad (1969). *Astrophys. J.*, **157**, 1465.
Kleinmann, D.E., and F.J. Low (1967). *Astrophys. J. Letters*, **149**, L1.
Larson, R.B. (1969a). *Mon. Not. Roy. Astr. Soc.*, **145**, 271.
Larson, R.B. (1969b). *Mon. Not. Roy. Astr. Soc.*, **145**, 297.
Larson, R.B. (1972a). *Mon. Not. Roy. Astr. Soc.*, **156**, 437.
Larson, R.B. (1972b). *Mon. Not. Roy. Astr. Soc.*, **157**, 121.
Larson, R.B., and S. Starrfield (1971). *Astr. Astrophys.*, **13**, 190.
Lin, C.C., L. Mestel, and F.H. Shu (1965). *Astrophys. J.*, **142**, 1431.
McCrea, W.H. (1957). *Mon. Not. Roy. Astr. Soc.*, **117**, 562.
McNally, D. (1971). *Rep. Prog. Phys.*, **34**, 71.
Mestel, L. (1965a). *Quart. J. Roy. Astr. Soc.*, **6**, 161.
Mestel, L. (1965b). *Quart. J. Roy. Astr. Soc.*, **6**, 265.
Nakano, T., and E. Tademaru (1972). *Astrophys. J.*, **173**, 87.
Narita, S., T. Nakano, and C. Hayashi (1970). *Prog. Theor. Phys.*, **43**, 942.
Neugebauer, G., E.E. Becklin, and A.R. Hyland (1971). *Ann. Rev. Astr. Astrophys.*, **9**, 67.
Newton, I. (1692). Letter to Bentley, quoted by J.H. Jeans in *Astronomy and Cosmogomy*, p.352, Cambridge University Press, 1929.
Nishida, M. (1968). *Publ. Astr. Soc. Japan*, **20**, 162.
Ostriker, J. (1964). *Astrophys. J.*, **140**, 1056.
Ostriker, J., and P. Bodenheimer (1973). *Astrophys. J.*, **180**, 171.
Penston, M.V. (1966). *Roy. Obs. Bull.*, No.**117**, 299.
Penston, M.V. (1969a). *Mon. Not. Roy. Astr. Soc.*, **144**, 425.
Penston, M.V. (1969b). *Mon. Not. Roy. Astr. Soc.*, **145**, 457.
Penston, M.V. (1971). *Contemp. Phys.*, **12**, 379.
Shu, F.H., V. Milione, W. Gebel, C. Yuan, D.W. Goldsmith, and W.W. Roberts (1972). *Astrophys. J.*, **173**, 557.
Spitzer, L. (1968a). In *Nebulae and Interstellar Matter*, B.M. Middlehurst and L.H. Aller (Eds.), University of Chicago Press, p.1.
Spitzer, L. (1968b). *Diffuse Matter in Space.* Wiley-Interscience, New York.
Spitzer, L., and E.H. Scott (1969). *Astrophys. J.*, **158**, 161.
Stein, R.F., R. McCray, and J.H. Schwartz (1972). *Astrophys. J. Letters*, **177**, L125.
Strom, K.M., S.E. Strom, and J.Yost (1971). *Astrophys. J.*, **165**, 479.
Strom, S.E., K.M. Strom, A.L. Brooke, J. Bregman, and J. Yost (1972a). *Astrophys. J.*, **171**, 267.
Strom, S.E., K.M. Strom, J. Yost, L. Carrasco, and G. Grasdalen (1972b). *Astrophys. J.*, **173**, 353.
Tsuji, T. (1971). *Publ. Astr. Soc. Japan*, **23**, 553.
Upton, E.K.L. (1968). In *Nebulae and Interstellar Matter*, B.M. Middlehurst and L.H. Aller (Eds.), University of Chicago Press, p.771.
Verschuur, G.L. (1971). *Astrophys. J.*, **165**, 651.
Walker, M.F. (1972). *Astrophys. J.*, **175**, 89.
Zeldovich, Y.B., and Raizer, Y.P. (1968). *Elements of Gasdynamics and the Classical Theory of Shock Waves.* Academic Press, New York.

Appendix A

THE DEPENDENCE OF THE RADIUS OF A STELLAR CONFIGURATION ON ITS SPECIFIC ENTROPY

It is often of interest to be able to understand in a simple way how the radius of a star is related to the conditions in its interior and how the radius varies as the star evolves. It is evident that for a star of given mass M, the radius R would be completely determined if it were possible to specify the density ρ at each point in the star; equivalently, given the equation of state and the condition of hydrostatic equilibrium, the same would be true if any other variable of state such as the pressure P or the temperature T were specified at each point. However, since the pressure, density, and temperature all vary by several orders of magnitude within a star, it is difficult to specify their distributions in any simple *a priori* way. There is, however, another variable of state, namely the entropy per unit mass s, which is generally more nearly constant throughout a star and whose value is in some cases more readily predictable. For example, if there exist adiabatic conditions (such as would exist in a convection zone) throughout part or all of a star, the specific entropy s is constant throughout the adiabatic region. In discussing the structure and evolution of the stellar core in a protostar of small or moderate mass it is convenient to make use of the concept of entropy, since radiative transfer is unimportant in such a core and each mass element therefore behaves adiabatically, conserving the entropy which it acquired on passage through the shock front. Since the radius of the core plays an important role in the evolution of the protostar, we consider the problem of relating the radius of such a stellar configuration to the specific entropy of the material in it.

Dimensional argument

Considering the simplest case of a perfect gas with constant specific heats c_p and c_v and with ratio of specific heats $c_p/c_v = \gamma$, the specific entropy s is given in terms of the pressure P and the density ρ by

$$s = c_v \ln(P/\rho^\gamma) , \tag{67}$$

apart from an additive constant which for present purposes can be taken to be zero. For a hydrostatic stellar configuration of mass M and radius R we have, dimensionally,

$$\rho \approx \frac{M}{R^3} , \qquad P \approx \frac{GM^2}{R^4} . \tag{68}$$

By combining Eqs. (67) and (68), we can express R as a function of s and M; we obtain, after simple algebra,

$$R \approx \left[\frac{\exp(s/c_v)}{GM^{2-\gamma}}\right]^{1/(3\gamma-4)} . \quad (69)$$

For the case of a perfect monatomic gas with $\gamma = 5/3$, Eq. (69) reduces to

$$R \approx \frac{\exp(s/c_v)}{GM^{1/3}} . \quad (70)$$

Thus we see that, dimensionally, the radius of a star can be considered to be a function of its specific entropy and its mass, and that R increases with increasing s and decreases with increasing M. Since the dependence of R on M is relatively weak, we see that it is primarily the specific entropy s which determines the radius of a stellar object.

Intuitively, the existence of a relation between the radius of a star and its specific entropy is not surprising in view of the fact that in statistical mechanics, the entropy of a system is a measure of the volume in phase space occupied by its constituent partcles; a higher entropy means that the particles are dispersed over a larger volume in phase space. Thus it is intuitively reasonable that a configuration of higher entropy, whose particles occupy a larger phase space volume, should also occupy a larger physical volume, i.e. have a larger radius.

Polytropic Models

From Eq. (67) we notice that the equation of state of the gas, considered as a relation between P, ρ, and s, can be written in the form

$$P = \exp(s/c_v)\,\rho^{\gamma} \quad (71)$$

which is closely analogous to the 'polytropic equation of state'

$$P = K\rho^{1+1/n} \quad (72)$$

on which polytropic stellar models are based. Thus we see that an isentropic configuration in which s and γ are constant throughout can be represented as a polytropic sphere with

$$K = \exp(s/c_v) , \qquad n = \frac{1}{\gamma - 1} . \quad (73)$$

The radius of a polytropic sphere of mass M is given by

$$R = \left[\frac{K}{N_n GM^{(n-1)/n}}\right]^{n/(3-n)} \quad (74)$$

(Chandrasekhar 1939), where N_n is tabulated by Chandrasekhar. Thus, substituting for K and n from Eq. (73), we obtain for the radius of an isentropic configuration with specific entropy s and ratio of specific heats γ

$$R = \left[\frac{\exp(s/c_v)}{N_n GM^{2-\gamma}}\right]^{1/(3\gamma-4)} . \quad (75)$$

Note that this is identical to Eq. (69) except for the constant N_n. In the case $\gamma = 5/3$, corresponding to a polytrope of index $n = 1.5$ (which is appropriate, for example, for a completely convective star), we have $N_n = 0.424$ and

$$R = 2.36\,\frac{\exp(s/c_v)}{GM^{1/3}} . \quad (76)$$

Thus if the specific entropy s (or equivalently, the quantity $P/\rho^{5/3}$) is known at any point in a convective star of given mass, the radius of the star is completely determined and has the value given by Eq. (76).

Discussion and comparison with models

In general, the above relations will not hold exactly, since the configurations of interest are not completely convective and s is not constant throughout. However, since the radius of a star is determined primarily by the structure of its outer regions and is relatively insensitive to the properties of the central region, one would expect the radius to depend mostly on the specific entropy of the outer layers of the star; the entropy of the central region should be much less important. This expectation is confirmed by looking at the structure of the stellar cores and pre-main sequence models described in this article and in previous investigations of pre-main sequence evolution; it is found that the radius is always more or less closely related to the specific entropy of the outer layers of the star, but is nearly independent of its value at the center. The relation between specific entropy and radius is particularly simple in the case of a star with a deep outer convective zone in which s is constant or nearly so (e.g., a star on the 'Hayashi track'); in such cases, Eq. (76) does, in fact, yield a reasonably close approximation of the radius of the star if s is taken

as the specific entropy of the convection zone. Thus, for example, the radii of various published pre-main sequence models with outer convection zones are generally predicted by Eq. (76) with an accuracy of about 5 to 10 percent, except for stars close to the main sequence where the convection zone becomes small, and stars with very large radii ($\gtrsim 30\,R_\odot$) in which the assumption of the constancy of s and γ breaks down in the outer layers. In the case of the stellar core in a collapsing protostar, Eq. (76) predicts the radius of the core with an accuracy of about 5 to 15 percent as long as the core has any appreciable outer convection zone.

Thus we see that, at least for protostellar cores and pre-main sequence stars, there is a close relation between the radius of such an object and the specific entropy of its outer layers, which is useful in discussing its structure and evolution. The existence of such a relationship makes particularly clear the importance of the shock front at the surface of the core for the evolution of protostars, since it is the properties of this shock front which determine the specific entropy of the material added to the outer layers of the core.

Fundamentals of Cosmic Physics, 1973; Vol.1, pp.71–118

Printed in Great Britain

Electron Plasma Resonances in the Topside Ionosphere

J. R. MCAFEE
National Oceanic and Atmospheric Administration, Boulder, Colorado 80302, U.S.A.

A very large variety of responses can follow rf pulses in the topside ionosphere. Most of those which can not be identified as normal electromagnetic echoes show a resonant-like behavior, or a ringing for times long after the exciting pulse. The general characteristics of the major ionospheric resonances, at the plasma, upper hybrid, and cyclotron harmonic frequencies, can be explained by treating the phenomena as one of electrostatic wave propagation and reflection. The well-developed theory for the resonances at the plasma and upper hybrid frequencies, presented in detail, may also point to similar explanations at the cyclotron harmonics and also at the maximum frequencies of the Bernstein modes. The theory not only provides a check on the dispersion relations for electrostatic waves, but raises the possibility of using the observations to measure electron temperatures. Some of the other resonant-like behavior, observed more sporadically, can be explained in principle by considering possible nonlinear effects. These include the low-frequency subsidiary resonances and the diffuse resonances, as well as the resonance at twice the upper hybrid frequency. Others, like the resonance at the cyclotron frequency and proton echoes are unexplained.

1 INTRODUCTION

Bottomside ionosondes have been a standard tool for ionospheric measurement and monitoring for many years. However, since radio waves return to the ground only from the portion of the ionosphere below the level of maximum electron density (bottomside), ionosondes provide no information about the ionosphere above this level (topside). With the advent of useful research satellites, it became obvious to put a sounder in orbit above this level to perform a function in the topside ionosphere entirely analogous to the bottomside sounders. Topside sounder satellites were then launched under the ISIS program (Jackson, 1965; Chapman, 1965; Calvert, 1966; Chapman